MURDOCH UNIVERSITY
PERTH, WESTERN AUSTRALIA

Thesis Report

Solar Collector Efficiency Testing Unit

A report submitted to the School of Engineering and Energy, Murdoch University in partial fulfilment of the requirements for the degree of Bachelor of Engineering.

Author: Hany Moussa

30415002

Unit Co-ordinator: Prof. Parisa Arabzadeh Bahri

Thesis Supervisor: Dr. Gareth Lee

27th February 2009

Murdoch UNIVERSITY

ABSTRACT

This Thesis report addresses some of the modifications implemented on a pre-existing project in aim to satisfy the 'Australian and New Zealand Standard AS/NZS 2535.1:2007' for a Solar Collector Efficiency Testing Unit. The prime objective of this assignment was to further improve on the performance of the testing unit by constricting the process parameter readings within the accuracy bounds quoted by the standard. Successful delivery of the project task will permit the testing unit to fulfil its intended purpose of allowing several tests to be conducted on the Solar Collector on a daily basis rather than the traditional one test per day arrangement.

The scope of this text provides careful analysis and adjustment procedures to certain aspects of concern that were believed to be potentially responsible for the existing accuracy failures. Thorough tests and experiments were conducted on all suspected factors of the setup as an empirical elimination process to ultimately identify which factors were causing the main concern in relation to accuracy.

Significant progress has been made on the accuracy limitation; however the results obtained suggest that it still marginally fails to abide within the bounds declared by the AS/NZS standard.

TABLE OF CONTENTS

TABLE OF FIGURES

TABLE OF EQUATIONS

TABLE OF TABLES

TABLE OF ACRONYMS

TT : Temperature Transmitter

FM : Flow Meter

T_{Mix} -TT : Mixed Stream Temperature Transmitter

HT - TT : Hot Tank Temperature Transmitter

CT - TT : Cold Tank Temperature Transmitter

HS - TT : Hot Stream Temperature Transmitter

CS – TT : Cold Stream Temperature Transmitter

CV : Control Valve

HS – CV : Hot Stream Control Valve

CS – CV : Cold Stream Control Valve

HS - FR : Hot Stream Flow-rate

CS - FR : Cold Stream Flow-rate

SSR: Solid State Relay

RTD – Resistance Temperature Device

W: Watts

J: Joules

1 INTRODUCTION

Solar collectors are special devices designed to extract electromagnetic energy from the sun and to efficiently transfer this energy directly to a more usable or storable form. There are several different types of solar collectors used today in homes and industries to cater for a variety of applications such as water heating or electricity generation. The design of a solar collector for water heating purposes usually consists of an insulated panel, fabricated with a black metal absorber sheet (for maximum energy absorption) containing in-built pipes. The collector also has an inlet and outlet terminal for water access through the pipes and is known to be called a “flat-plate collector”. Once the solar collector is mounted facing the sun, an inlet water feed supply continuously circulates though the hot pipes which allows efficient heat transfer to the water. The heated water in the pipes is then fed through the outlet terminal of the solar collector which can be subsequently directly used or stored in an insulated reservoir. A domestic application of a solar collector can be to heat water for a swimming pool or to provide heat in a hot water tap. So far, solar collectors have been discussed through the context of heat transfer through liquid water, however not all solar collectors use water as their heat transfer medium. Another type of a solar collector known as the “Solar Pyramid” (Wikipedia, 2009) is designed to heat air from solar energy and pass the air through turbines to generate electricity. This type of solar collector can be found in industrial plants within Australia and India.

The efficiency of a solar collector can be defined as “A Measure of the ratio of energy removed from a specified reference collector area by the heat transfer fluid over a specified time period, to the solar energy incident on the collector for the same period” (Standards Australia, 2007). There are numerous factors which may affect the efficiency of a solar collector such as the type of material used and thermal loss from the pipes. However, these factors lie outside the scope of this project. Upon testing the efficiency of the collector, the inlet water temperature and flow rate must be controlled within strict accuracy bounds so that when it is compared with the heated outlet stream, an accurate measure of the efficiency can be deduced.

Murdoch University (South St. Campus) currently has a solar collector testing unit apparatus that features a large water tank to supply continuous water feeds to the solar collector for efficiency testing purposes. However, there is one main disadvantage to this structure which is the amount of time required to heat the water in the tank. As a result, this allows only one test to be conducted per day since the water in the tank had to be pre-heated one night in

advance of test execution. The problem with this setup is that although the scheme successfully performs its required task, which is to test the efficiency of the solar collector, it fails to provide time efficiency. In consequence, the proposal of this project was developed as an alternative routine intended to allow several tests to be conducted on the solar collector during any sunny day, by a faster water heating process.

In 2006, Phil Minissale and Huang Jian, both former Murdoch University students, designed a system that will supply a water feed, to a solar collector at a range of different temperatures and flow rates, in an attempt to effectively satisfy the proposal. The aim of the project was intended to comply with the Australian and New Zealand standard of testing the efficiency of a collector. The standard of testing state that the system must be capable of supplying the final mixed feed to the solar collector at an accuracy of ± 0.1° in terms of temperature, in conjunction with a ± 1% precision for the feed flow-rate (Standards Australia, 2007). The outcome of the system failed to meet the accuracy criteria of the given standard for several reasons which were investigated one year later by the next operator, Hamad Al-Senaid, who focused his efforts on modifying the pre-existing system to ultimately resolve these accuracy issues which violated the standard. Al-Senaid introduced some new modifications to help improve the accuracy issues which he could not resolve. These suggested modifications will also be addressed and explored through the various chapters of this report.

This text reveals a thorough analysis that includes a review of previous examinations and outcomes, System design architecture, implemented Control schemes, instrument calibration, hardware and software descriptions and most importantly the empirical elimination processes conducted to fulfil this project's major aim.

The outcomes of the experimental results exposed in this report indicate that the resultant inlet feed supply still slightly fails to conform by the standard, for reasons justified though the empirical analysis examined in this text.

2 PROJECT HISTORY

2.1 PREVIOUS SETUP CONSTRUCTION

The evolution process of this system has become quite intense since its original establishment in 2006. The setup is comprised of two water tanks that are provided with water feed from a common supply. Both tanks were fitted with a heating element and a recycle stream to regulate the water temperature to a desired degree. The outlet flow streams from each tank are then combined to create the resultant flow-rate and temperature required for the solar collector inlet. A schematic diagram representing this system is shown below in figure 1.

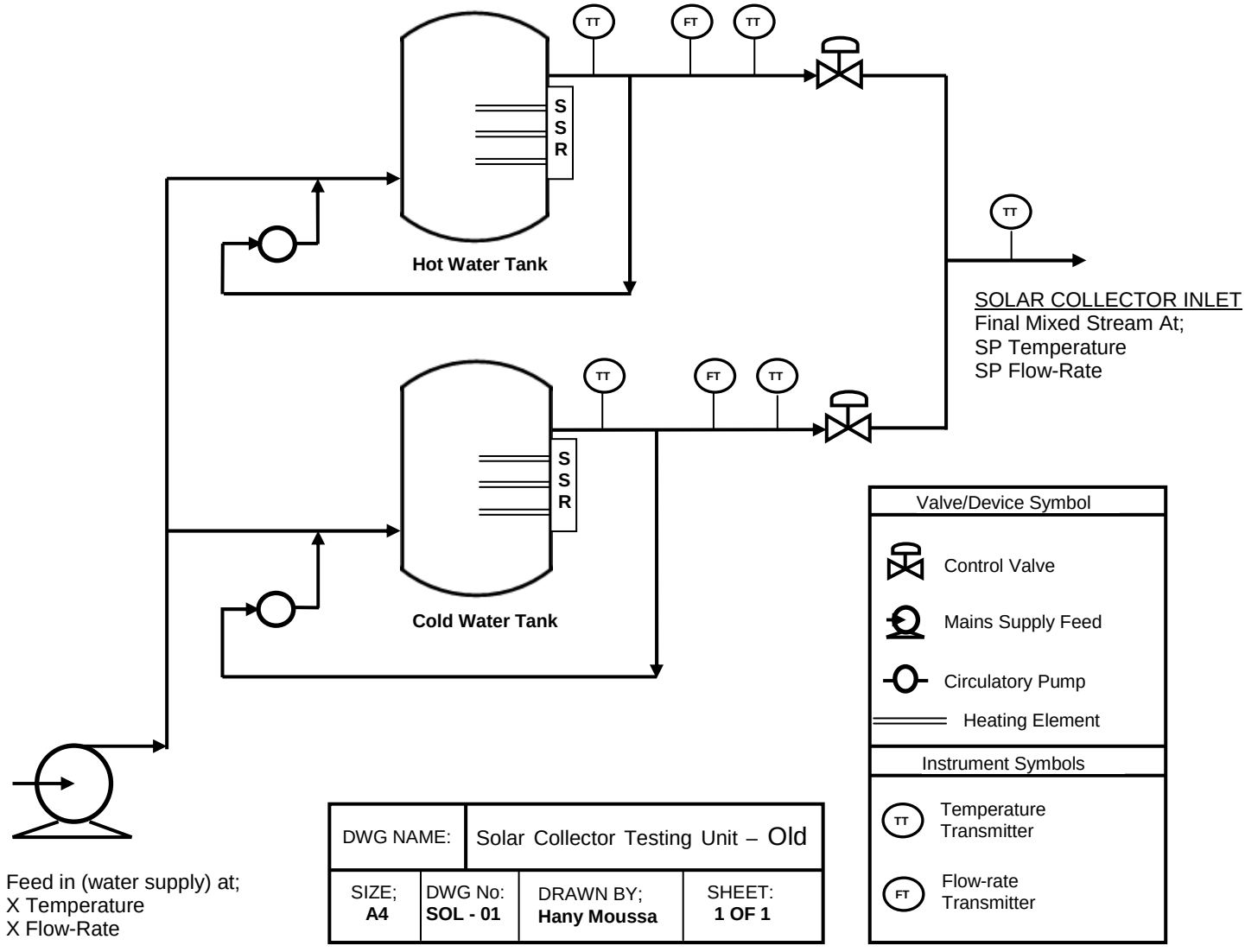

Figure 1: Previous Schematic diagram of System Process

There are two temperature sensors placed immediately at the outlet of each tank to indicate the water temperatures inside each tank. All the Resistance Temperature Devices (RTD) are mounted on pipes with the assumption that the pipe temperatures are equivalent to the water temperatures flowing through them. Two flow transmitters are placed down-stream to measure the flow-rates on each stream. The flow devices are placed within a small proximity to the control valves for accurate flow-rate control. This was deliberately done as both streams combine shortly after. There are also two temperature sensors mounted immediately before the control valve to determine the water temperature at each stream. Once again, this arrangement allows the control valves to make further adjustments for accurate control, before the temperatures of each stream subsequently mix. The final RTD is situated at the solar collector's input feed, to monitor the temperature of the water entering. The temperature reading of this sensor is of most importance as it is expected to comply with the accuracy of the AS/NZS standard (Standards Australia, 2007). The three heating elements in each tank are power rated at 4800W each, accumulating a potential total of 14,400W of power to each tank. The system is completely computer controlled by data acquisition through field point modules. A detailed description and functionality of all the devices and sensors used, are reviewed in the 'Physical devices' chapter.

2.2 PREVIOUS CONTROL STRATEGY

The structure provided in the schematic diagram of figure 1, is classified as a "Multiple Input Multiple Output" (MIMO) system as there are two manipulated variables (cold/hot flow-rates) to control two process variables (Final temperature and flow-rate). There is an existing complication with MIMO systems, which is not apparent with a Single Input Single Output (SISO) system. The problem with MIMO systems is that one manipulated variable usually affects more than one process variable, which consequently calls upon on a more complex control strategy. This phenomenon is referred to as "Process Interaction" and is common with almost all MIMO systems (Ogunnaike, 1994 pg. 684-686).

The system designed in the schematic diagram of figure 1, proves to exhibit process interaction because varying the flow-rate of either stream will not only affect the final flow-rate, but the temperature in consequence. Figure 2 represents the diagram of the pre-existing control scheme.

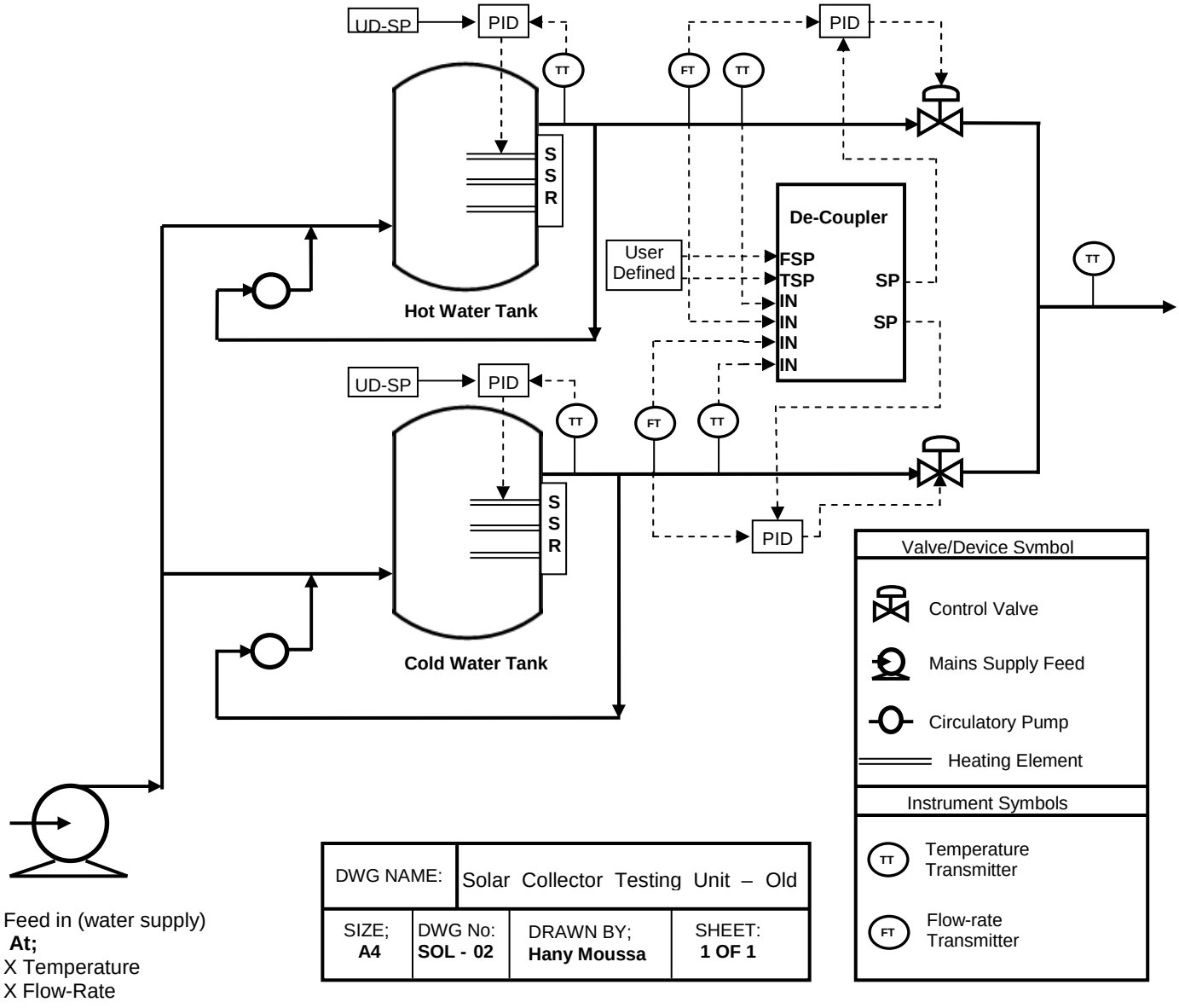

Figure 2: Old Schematic diagram of Control Scheme

The immediate question to be raised when dealing with a MIMO system is "*which input variable should be used in controlling which output variable?*" (Ogunnaike, 1994 pg 684-686). To treat this issue, a Relative Gain Array (RGA) analysis is usually performed to reveal the appropriate looping pairs by calculating which manipulated variable affects which process variable the most. A separate control approach has been taken by the original author of this project because both manipulated variables affect the process variables equally, which is the worst case of process interaction. This leads to the alternative control scheme of the de-coupler mentioned below.

2.2.1 De-coupler Implementation

The de-coupler block consists of a mathematical algorithm designed to calculate theoretical flow-rate set-points for each stream which will consequently satisfy the desired temperature and flow-rate set-points at the solar collector input. The set-points from the de-coupler are sent to both PID controller loops wrapped around both the hot and cold streams.

The output set-point calculations for both streams are derived by the following mathematical functions;

Set-point calculation for Cold Flow-rate Stream;

$$\mathbf{CF_{SP}} = \mathbf{F_{SP}} \frac{\mathbf{T_H} - \mathbf{T_{SP}}}{\mathbf{T_H} - \mathbf{T_C}}$$

Equation 1: Cold Stream Flow-rate SP

Set-point calculation for Hot Flow-rate Stream;

$$\boldsymbol{HF_{SP}} = \boldsymbol{F_{SP}} \frac{\boldsymbol{T_{SP}} - \boldsymbol{T_C}}{\boldsymbol{T_H} - \boldsymbol{T_C}}$$

Equation 2: Hot Stream Flow-rate SP

Where;

F_C = Cold Stream Flow-rate
F_H = Hot Stream Flow-rate
T_C = Cold Stream Temperature
T_H = Hot Stream Temperature
F_{SP} = Final Mixed Stream Set-point
T_{SP} = Final Mixed Temperature Set-point

(Al-Senaid, 2007)

Temperature control for this de-coupling scheme is not directly dealt with in terms of a control loop because it is maintained by the combination of the flow-rate set-points. That is, if the calculated flow rate set-points are met, then the desired mixed stream temperature will automatically be met in turn, assuming no heat loss occurs in the downstream pipes where the streams combine. The equations above work based on the assumption that the steams will mix perfectly and can be theoretically determined by the equations represented below;

Final Mixed Temperature Equation;

$$\boldsymbol{T_M = \frac{(F_C T_C) + (F_H T_H)}{(F_C + F_H)}}$$

Equation 3: Final Mixed Temperature Equation

Final Mixed Flow-rate Equation;

$$\boldsymbol{F_M = F_C + F_H}$$

Equation 4: Final Mixed Flow-rate

2.2.2 De-coupler validation

To be convinced that the de-coupler correctly works, a trivial theoretical calculation will be performed below to test its validity.

If the user was to request a final mixed water temperature of 40°C flowing at 3 litres/min, the following calculation below will determine the flow-rates at which each stream must meet to satisfy these conditions.

Assuming these initial conditions;

- Water in hot tank = 60°C – then T_H = 60°C (hot stream temperature)
- Water in Cold tank = 20°C – then T_C = 20°C (cold stream temperature)
- T_{SP} = 40°C (desired Final mixed temperature)
- F_{SP} = 3 l/min (desired Final mixed flow-rate)

Substituting the values above into equation 1:

$$CF_{SP} = 3\frac{60-40}{60-20} = 1.5\ l/min$$

Equation 5: Cold stream flow-rate set-point example calculation

Substituting the values above into equation 2:

$$HF_{SP} = 3\frac{40-20}{60-20} = 1.5\ l/min$$

Equation 6: Hold stream flow-rate set-point example calculation

The calculations suggest that if a flow-rate of 1.5 l/min at 20ºC from the cold stream was to mix with flow-rate of 1.5l/min at 60ºC from the hot stream; this would produce a final flow-rate of 3 l/min at 40ºC as the user has requested. This is conceptually true as the final temperature would settle to the equilibrium point of 40ºC if equal parts of water from each stream are to mix.

Substituting the values into Equation 3:

$$T_M = \frac{(1.5 \times 20) + (1.5 \times 60)}{1.5 + 1.5} = 40°C$$

Equation 7: Equilibrium temperature justification

This equation is used to determine the equilibrium temperature of two streams that mix at the given flow-rates and temperatures. The above calculation proves that a flow-rate of 1.5 l/min from each stream will result in a final mixed temperature of 40ºC.

Substituting the values into equation 4:

$$F_M = 1.5 + 1.5 = 3\ l/min$$

Equation 8: Combination Flow Justification

This equation simply proves that the addition of both flow-rates is equivalent to the final flow-rate.

2.3 RESULTS AND OUTCOMES

Al-Senaid conducted a few tests to analyse the steady-state accuracy of the final flow-rate and temperature. The tests were performed under the conditions stated below:

- Water in hot tank = 70°C
- Water in cold tank = 25°C
- F_{SP} = 3 l/min – as this was recommended by the AS/NZS standard, (Standards Australia, 2007).

Two of the temperature set-points chosen were 55°C and 60°C. The statistical data in the tables below indicates the system performance at that time.

Flow-rate at 55°C	
Mean	3.002115
Median	3.002
Mode	2.997
Standard deviation	0.026968
Kurtosis	0.017745
Skewness	0.215407
Minimum	2.937
Maximum	3.101
Sample variance	0.000727

Table 1: Old Flow-rate statistics at 55°C

Temperature 55˚C	
Mean	54.8778
Median	54.886
Mode	54.886
Standard Deviation	0.108557
Kurtosis	0.908257
Skewness	0.384482
Minimum	54.597
Maximum	55.372
Sample Variance	0.011785

Table 2: Old Temperature statistics at 55°C

Flow-rate at 60°C	
Mean	3.0045
Median	3.005
Mode	3.003
Standard Deviation	0.02186
Sample Variance	0.00048
Kurtosis	-0.5951
Skewness	-0.0519
Minimum	2.937
Maximum	3.05

Table 3: Old Flow-rate statistics at 60°C

Temperature 60˚C	
Mean	59.7184
Median	59.695
Mode	59.578
Standard Deviation	0.28413
Sample Variance	0.08073
Kurtosis	-1.0344
Skewness	0.12871
Minimum	59.17
Maximum	60.275

Table 4: Old Temperature statistics at 60°C

(Al-Senaid, 2007)

The results above indicate that accuracy performance for this system severely lie outside the boundaries required by the standard, as the minimum and maximum values of the flow and temperature readings were to never exceed ± 1% and ± 0.1°C respectively. Al-Senaid argued that the flow readings were noisy; therefore the standard deviation measurement should be considered for determining the system's performance. The standard deviation is a measurement of how far the values are away from the mean, which would eliminate the effect of the noise factor as all values would be averaged.

Another point Al-Senaid raised was that the flow valves incurred "hysteresis" which was previously proved by Eric (Jian, 2006). Al –Senaid defined valve hysteresis as "The dynamic response to the change that causes the path of movement of the valve stem to be different when the response is increasing that when the response is decreasing". He justified this claim by saying that when a signal was sent to the cold valve to open, the valve would become "sticky" and therefore hesitate to move. This consequently provoked the de-coupler to slightly open the hot stream valve to satisfy the ultimate flow-rate set-point defined by the user. However, doing this caused an inappropriate increase in temperature for the final flow. After this incident had occurred, the cold valve would finally overcome the "stickiness" with an abrupt force causing it to overshoot. This event would further oblige the de-coupler to calculate new set-points. The ultimate effect of this hysteresis issue caused substantial fluctuations for the final flow and temperature, which is evident in the minimum and maximum readings portrayed in the results above. Al-Senaid concluded that the valves needed to be changed to improve system performance.

3 PROPOSED MODEL

3.1 CURRENT SETUP CONSTRUCTION

There was one forced alteration made to the physical structure due to a heater hardware failure. The heater in the hot water tank malfunctioned somewhere between project handover thus alternative architecture was constructed as seen in figure 3.

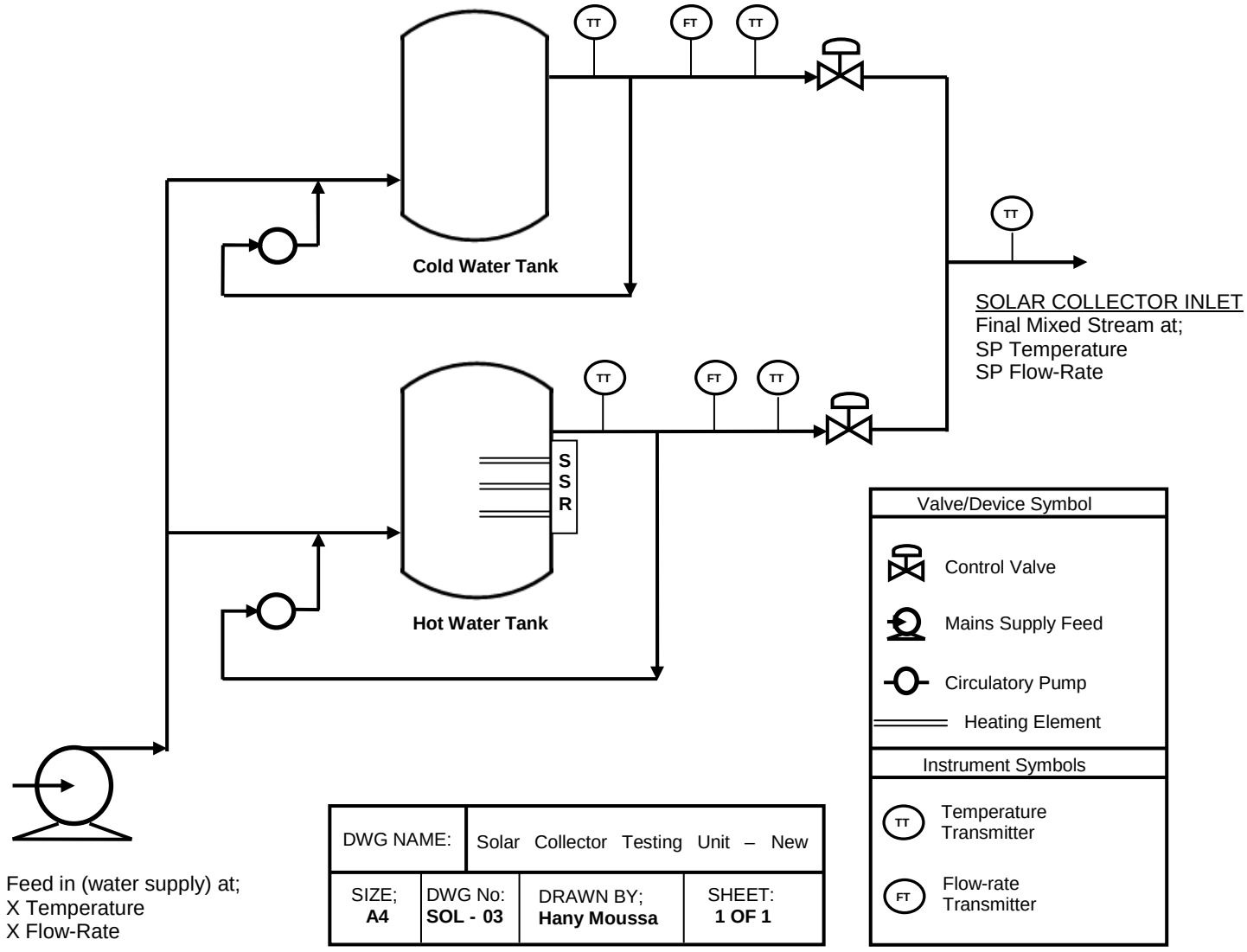

Figure 3: Current schematic diagram of system process

As can be viewed from the system above, the water tanks have switched identities having the hot water tank on the bottom with the cold water tank on the top. The cold water tank temperature is determined by the ambient supply feed temperature. This system adjustment did not change any of the process characteristics hence no further performance complications were introduced.

3.2 CURRENT CONTROL STRATEGY

Minor changes have been made to the control strategy. The de-coupler has been kept but an additional PID loop has been implemented and represented below in figure 4.

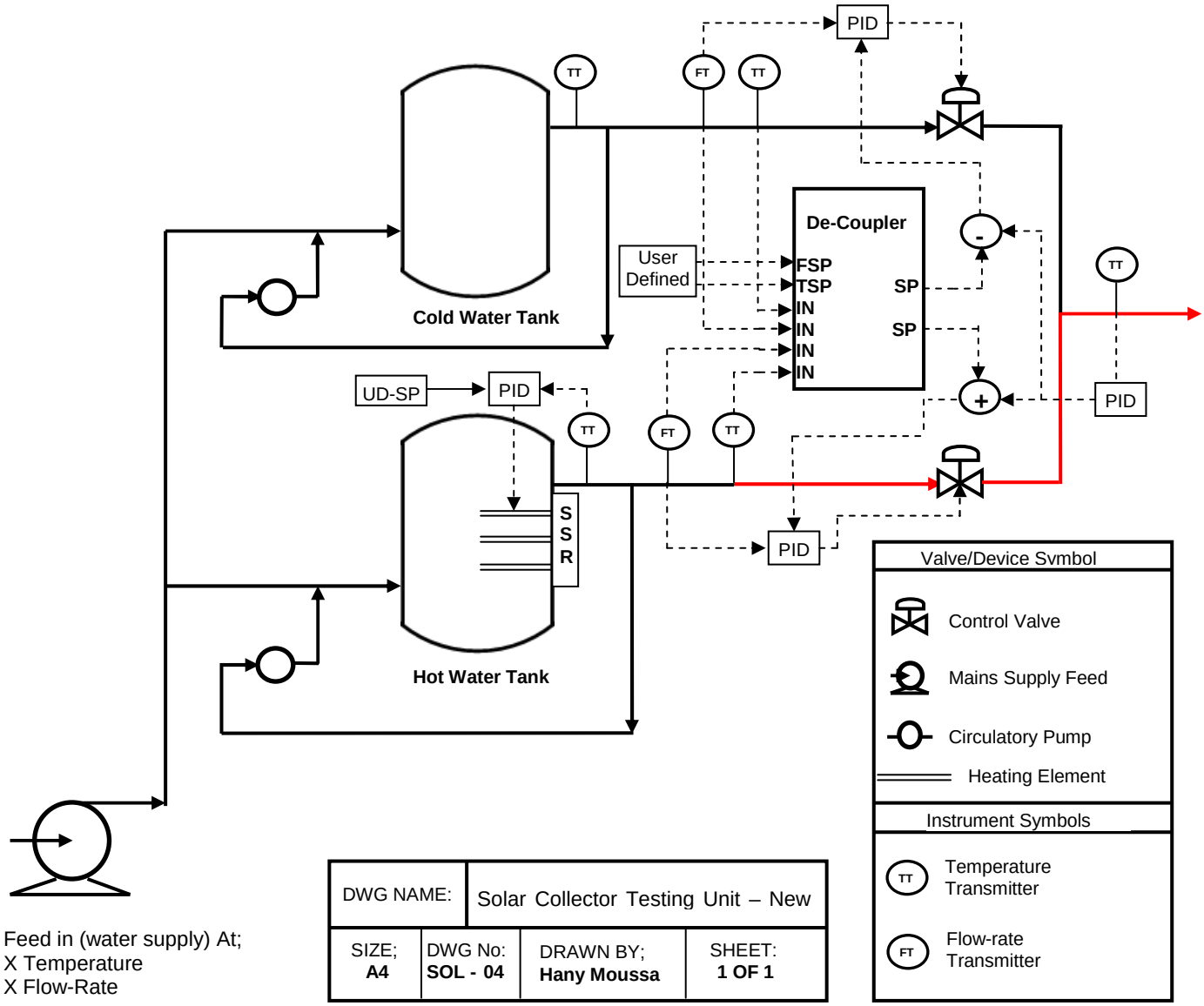

Figure 4: Current schematic diagram of control scheme

The red lines above represent heat loss in the hot stream pipe. Due to the fact that the de-coupler does not account for radiant heat-loss after the hot stream temperature sensor, an extra PID loop was placed to adjust the hot stream set-point by a small additional percentage and minus the cold stream set-point by the same magnitude. Consequently, the final flow-rate is unchanged and the negative temperature offset that previously existed, was removed. More on this topic is discussed within the “Project Adjustments” chapter of this report.

3.3 INSTRUMENT MODIFICATIONS

As previously mentioned, the need for replacement valves was suggested by Al-Senaid due to the hysteresis issues that were presented with the original valves. The 'Baumann' open/close valves were pneumatically controlled by a 4-20mA control signal and were tested to be non-linear. The graph in figure 5 below was created by Jian to represent the characteristic curve for the hot stream control valve.

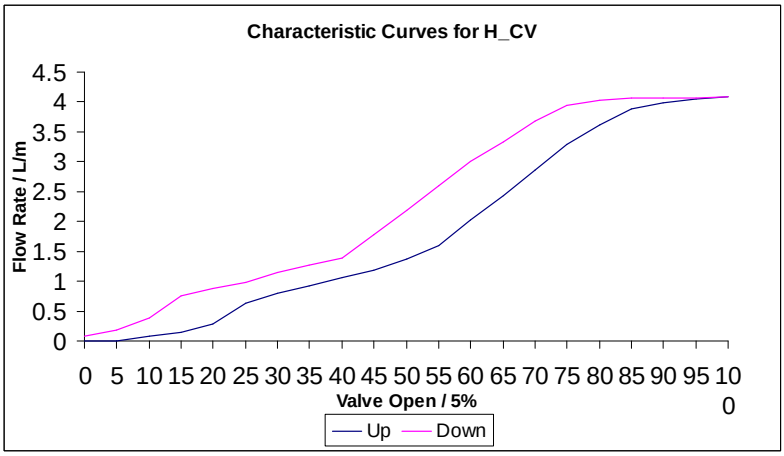

Figure 5: Hot stream control valve characteristic curve

The hot stream control valve was stepped up from 0 to 100% in 5% intervals then back down respectively. There is a clear nonlinearity between the opening percentage and the flow-rate. This valve characteristic method is a great test to identify any hysteresis evident in the valve. If both lines on the graph above were exactly on top of each other, then this would suggest that the valve does not exhibit any hysteresis because the flow-rates would be identical for any given valve position. Thus the graph above suggests valve hysteresis because the flow-rates differ by more than 5% for the corresponding valve positions in reference to the blue and pink line.

This issue creates a motivation for the search of alternative replacement valves, as a modification action to improve the system's performance. The valve search was not a trivial task, as careful analysis had to be made on candidate valves to ensure a safe investment was made on an appropriate product. The search process was to discover a set of valves that would meet the desired criteria presented below:

- Hysteresis free
- Port size = ¼ inch
- C_V = 0.6 or less

- Can be controlled via a 4-20mA signal
- Supports a 0-4 l/min flow-rate
- Sufficient resolution accuracy (1/2 percent or less)
- Within University budget

Two Perth based process equipment and instrumentation companies were contacted via telephone and email for advice on valve type selection and pricing. Unfortunately, both companies failed to return any queries or offer any advice as promised. This is a common problem with university students trying to interact with companies for advice, as most companies are busy with 'real' clients. Nonetheless, the search process continued to progress with the final verdict being between "proportional control valves" and a "mixing valve". A discussion on both these valve types will be presented below.

3.3.1 Proportional control valves

Proportional control valves are valves that are positioned proportional to the input signal. This signal could be a 4-20mA or a 0-1.5VDC signal. The 'Baumann 51000' valves originally implemented on the system were proportionally controlled by a 4-20mA signal via pneumatic actuation.

The Hass Manufacturing Company located in America is an instrumentation organisation that specialise in valving products. The **EPV-250B** proportional control valve was discovered with the following specifications:

- Maximum $C_V = 0.6$
- 1/4 inch port size
- Linear flow characteristics
- 4-20mA or 1.5VDC input
- No backlash or hysteresis
- DC step motor 200 steps/rev
- 4 revolutions for full stroke
- 1/2 percent resolution 200:1
- Requires 12-24VDC power
- 5 year warranty

$385.00 US

(HMC, 2009)

Figure 6: EPV – 250B Control Valve

The EPV – 250B proportional control valve specifications had met all the desired criteria, promising a 0.5% resolution in conjunction with no backlash or hysteresis which was very attractive. Its price was also very reasonable making it a considerable candidate for the final product decision.

(HMC, 2009)

3.3.2 Mixing control Valve

Mixing control valves are valves that are designed to accurately control water temperature by an onboard highly complex control algorithm. The control valve comes in one unit with two input ports for a hot and cold stream, and one output port which is the product of the streams. The next type of control valve analysed was the **"Intellifaucet RK 250"** also made by the Hass manufacturing company. The List of its specifications is detailed below:

- Maximum C_V = 0.6
- 1/4 inch port size
- 4-20mA or 1.5VDC input
- No backlash or hysteresis
- 4°C - 60°C Temp Operation
- Temperature accuracy of ± 0.1℃
- Valves repositioned 60 times per second
- Fully automatic control
- Requires 12-16VDC power
- 0 – 19 liters/min
- 5 year warranty

$1345.00

(HMC, 2009)

Figure 7: RK 250 Control valve

The beauty of the mixing valve above is that it promises temperature accuracy control within ± 0.1℃ which meets the standard requirements. The mixing valve features an onboard high-speed micro computer that repositions two motor driven valves at an unbelievable rate of 60 times per second. The valve also claims that it is able to keep the output temperature constant even with pressure and temperature fluctuations in the hot and cold input streams. There are two disadvantages for this mixer. The first downfall is that the mixer can operate with a maximum input temperature of 60℃. The final flow-rate temperature suggested by the standard should be between 20℃ - 70℃ which is una chievable by the mixer. The second

downfall is that is that temperature control is its primary function, leaving flow volume as a secondary function with an unknown accuracy bound. This information implies that this mixer may or may not meet the terms of satisfying the ± 0.1% flow-rate bound requested by the standard. To treat this issue, one EPV-250B proportional valve may be purchased and placed at the exit stream of the mixing valve to control the final flow-rate. The schematic representation in figure 8, demonstrates how this can be achieved.

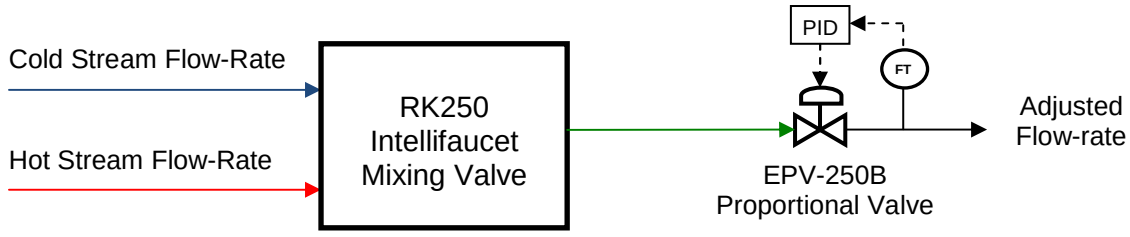

Figure 8: Mixing Valve Flow-rate Adjustment diagram

The process above illustrates the hot and cold stream flow-rates coming from each tank and into their ports on the mixing valve. The outlet stream temperature is accurately adjusted to the desired set-point but the flow-rate may still be inaccurate. The resultant stream then passes the EPV-250B proportional valve for flow-rate adjustment before it is to enter the solar collector.

The final verdict was to purchase a set of ‘EPV-250B’ and the ‘RK 250’ mixing valve but with a specialised integrated chip to allow for higher temperature inputs than the maximum stated in its specification. The idea was to implement the proportional control valves in place of the Baumann pneumatic valves and test the system’s response. If the proportional valves were found to be incapable of the task, then the alternative control strategy above would subsequently be implemented to achieve the task.

The proportional control valves were in fact used for the duration of this project as they were not considered to be responsible for the mixed stream inaccuracies. More on this topic is mentioned in the “Results” chapter of this report.

4 EQUIPMENT AND DEVICES

4.1 PHYSICAL SETUP DEVICES

The solar collector testing unit setup strictly consists of the following devices:

- Two water storage tanks
- One heating Unit
- Two circulatory Pumps
- Two Electromagnetic Flow meters
- Two Proportional control valves
- Five temperature sensors

4.1.1 Water Storage Tanks

The 'Rheem' storage tanks have a maximum volume of 50 litres with a maximum working pressure rated at 1000kPa. They are mounted on top of each other, with an insulation layer between them to avoid any heat transfer to occur. Each tank has an inlet port situated near the bottom and an outlet port at the top.

4.1.2 Heating Unit

There is one working heating unit located inside the hot water tank. The unit consists of three heating elements rated at 4800W each which combine to produce a maximum power of 14,400W. A thermostat installed by the manufactures was intended to control the water temperature in the tank between the range of 60℃ and 82℃. However, this thermostat has been disconnected to allow the user to vary the temperature of the water by a Pulse Width Modulation (PWM) signal produced by the 'PWM-520' Field point module. The signal is sent to three Solid State Relays (SSR) mounted on the heating unit. All three heating elements are bridged and thus activate simultaneously. Water in the hot tank is required to be no less than 70℃ which is only satisfied when the heating unit provides full power. Further discussion on this topic is reviewed in the "Project Adjustments" chapter.

4.1.3 Circulatory Pumps

There are two circulatory pumps mounted at the immediate outlet of each tank. Their objective is to continuously circulate the water from the outlet stream and back into the inlet stream. The purpose of the pumps is to ensure uniform heat distribution for the water in the

tank. The pumps are manufactured by 'Davey Pumps' and each require 230VDC power supply to operate. There are three selectable motor speeds to suit the users' application. The first speed operates at 1000 Revolutions per Minute (RPM) providing 45W of power. The second speed runs at 1450RPM with 66W of power, while the third speed functions at 1950RPM with 89W of power. The faster the motor is turning, the more accurate the heat distribution becomes in the tank.

4.1.4 Flow Meters

The 'Promag 10H' flow meters developed by "Endress + Hauser," are the current flow measuring devices employed for this system. The flow meters are mounted just before the valves on each stream in a horizontal position. The manufactures of this product also advised that correct measurement is only possible if the pipe is full and rated the maximum measured error to be ± 0.5%. These flow meters have a power requirement of 24VDC and output a 4-20mA current signal proportional to a 0-4 litres/ min flow. The meters also feature a user friendly human interface to allow the operator to change various settings such as process system parameters. There is a default security encryption on the meters that forbid the user from changing any settings. The default password is "1000". More information on these flow meters can be found in [App.D].

4.1.5 Temperature Sensors

As mentioned earlier in the "Project History" chapter of this report, there are currently five temperature sensors mounted to monitor flow-rate temperatures at various positions. The type of RTD's used were 'PT-100,' and can detect temperatures ranging from 0-150℃ that are proportionally outputted though a 4-20mA signal. The temperature readings from the sensors can be verified though the resistance table in [App.D] which indicates the acceptable temperature readings for the corresponding resistance values. In 2006, Phil Minissale conducted empirical tests on these sensors and concluded that they had an accuracy of ± 0.15%. Further analysis on this matter is presented in the 'Instrument Calibration' section of the text.

4.2 FIELD POINT MODULES

Field-point Units are devices that are commonly used in the industry as a means of data acquisition between field devices and a PC. They allow the user to read and write analogue/digital signals from the field and vice versa. Five field point modules were used for this project to control the system with all wiring diagrams illustrated in [App.A]. A detailed description and purpose for each module is presented below:

4.2.1 FP-1000

The 'National Instruments FP-1000' module was the device that interfaced with the PC via a RS-232 serial link. This module is responsible for gathering data from all the other field point modules and sending it through to the PC. Its other objective is to collect data written from the PC and send it to the intended field point addresses. The FP-100 is mounted behind the setup on a DIN rail and is capable of connecting with 25 other field point banks. The baud rate setting for this device ranges from 300 – 115200kbps but was set to the maximum for fastest data transfer. This module requires a 24VDC power supply that activates all other modules connected to it.

4.2.2 FP-AI-110

This module has 8 input channels which can read both voltage and current signals but is currently set to measure all analogue input signals by 4-20mA current loop. It features an impressive 16 bits of resolution and contains an in-built low-pass filter that is user configurable for 50-60Hz noise rejection. The module currently reads in the temperature from the hot and cold water tank sensors. Two other signals were intended to be attached to this module which were the 'wind velocity' and 'collector irradiance' measurements. However, the devices for these signals were not available. Measurement Readings of these devices are already accounted for in the LabVIEW program hence retrieval of these devices becomes a matter of simply connecting them to their allocated channels.

4.2.3 FP-AI-111

This module has the same specifications as the module above with the exception that it contains 16 input channels that only read 4-20mA current signals. The signals presently connected to this module are the temperature and flow transmitters on each stream along

with the final mixed stream temperature transmitter. Three additional temperature sensors are intended to be connected to this module when this system is to interface with the solar collector. One additional temperature sensor is required to measure the ambient atmospheric temperature, while the other two are required to read the solar collector inlet outlet temperature respectively. Once again these sensors have already been accounted for in the LabVIEW program and it is only a matter of connecting them to their allocated channels to achieve the fully functional system.

4.2.4 FP-AO-200

The FP-AO-200 has 8 current output channels and contains 12 bits of resolution. This module has two output ranges which are 0-20mA or 4-20mA and is generally used in the industry to control valves, gauges and other industrial actuators. The application of this module for the existing system was used to vary the valve gate position on each stream to ultimately control the flow-rate. The LabVIEW PID output signals ranged from 0-100% which was then scaled to a 4-20mA current signal.

4.2.5 FP-PWM-520

The FP-PWM-520 module has 8 voltage output channels that can supply 5, 12 and 24VDC at a maximum current of 1 amp. The device outputs PWM at frequencies of up to 1 kHz with a duty cycle range of 0-100%. A 12V output signal from this device was connected to the SSR's of the hot water tank heating element for water temperature control.

4.3 ADDITIONAL REQUIRED EQUIPMENT

Assembling the existing system required some additional equipment which was necessary to gain for the system to run. The table below provides a summary of all the extra equipment gathered and its purpose.

Equipment	Qty	Purpose
24V power supply	5	2x Power to flow-meters 2x power to EPV-250B Valves 1x Power to FP modules
12V power supply	1	Power up PWM-520 FP module
4mm sockets	4	To connect FP Comm. device to external power supply
Wires	5m	To power FP modules/Instrument signalling
Multi-meter	1	Voltage/Current measurements
Screw driver	1	To connect wires to FP ports

Table 5: List of Additional Equipment Required

4.4 PC AND SOFTWARE PACKAGES

4.4.1 PC + Specifications

One PC was required for this project and was used to control the system through the pre-written LabVIEW program discussed in chapter 5. The PC used had a Windows XP operating system and a serial port for field point connection. Advanced PC specifications are important as a small loop time is used in the LabVIEW program (250ms). The PC that operated the system is recommended for future use and thus had the following specifications:

- Intel Core 2 Duo
- 2.33 GHz CPU
- 3.25GB RAM
- Windows XP Professional

4.4.2 Automation Explorer

The National Instruments Automation Explorer software package was used to establish and configure a Field-point library by detecting all Field-point modules attached via the RS-232 port. The software allows the user to directly read or write signals to the field devices to verify signal readings. All analogue inputs and outputs were scaled from the real process variables into a 4-20mA current signal. Input readings on Automation Explorer can be switched between the real process variable and the proportional scaled current version. The user is encouraged to switch between both settings to confirm if scaled values are being displayed correctly. All configuration settings are saved in the 'Solar Tester Project.iak' file located in the 'Project Files' folder on the CD.

4.4.3 LabVIEW

The National Instruments LabVIEW 8.0 software package is required to run the system's LabVIEW program. The package must also have the 'Field-point I/O' add on module to detect field-point devices.

5 LABVIEW PROGRAM AND GUI

The pre-designed LabVIEW program allows the user to monitor, control and record data from the system. This text will highlight some of the modifications that have been made on the block diagram and front panel screens of the pre-existing program that was originally created by Phil Minissale in 2006.

5.1.1 Block diagram

The following modifications were implemented on the block diagram;

1. The first major adjustment made in the block diagram was deleting the PID control loop around the cold tank as this was found to be unnecessary since the water could only be at ambient temperature. This meant that the ambient water temperature reading of the cold water stream was continuously sent to the de-coupler.
2. The second modification made to the block diagram was replacing all the PID sub VI's with alternative blocks that supported an auto/manual mode. This allows the user to de-activate the control loops while the program is running, and manually write values to change the valve positions on each stream. This modification was necessary to allow the user to examine the valve characteristics.
3. The third main alteration made in the block diagram was the implementation of the additional PID controller that was wrapped around the final mixed temperature sensor and the hot stream flow-rate to eliminate the temperature offset that was occurring in the final mixed stream.
4. The Fourth central modification was made in the data logging program which allowed the hot and cold stream flow-rates to be logged. This was done so that the controller behavior can be graphically examined after running a set-point test.

5.1.2 Front Panel

There are still three front panel user selector screens that provide information about the system. The control parameters screen was slightly altered to provide graphical information for the hot and cold stream flow rates. The image below illustrates the current control parameters screen;

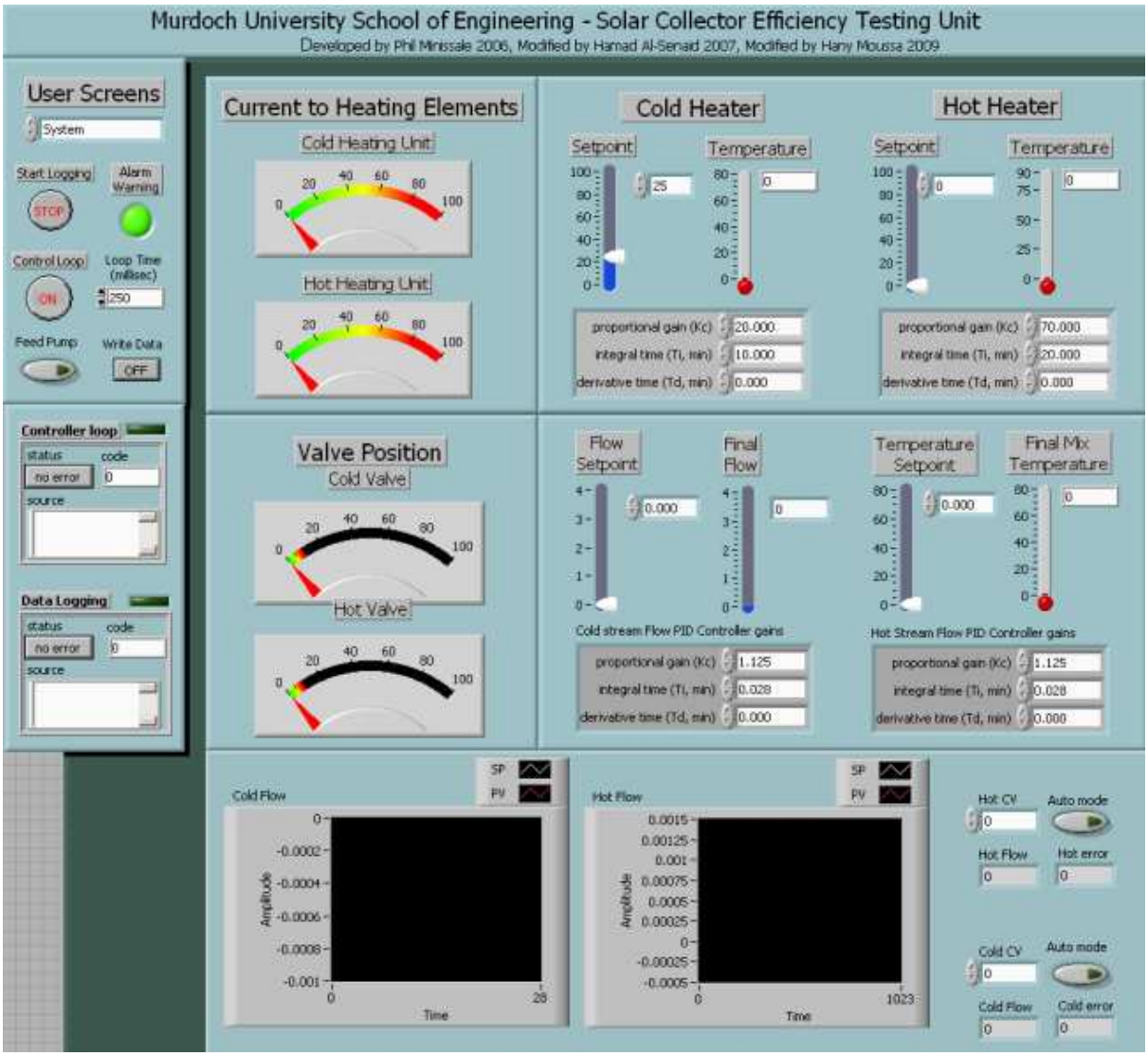

Figure 9: Front Panel - Modified Control Parameters Screen

The image above represents the new control parameters screen. The cold heater PID panel was not removed in case the heating element gets recovered. However, this panel currently has no effect on the overall system. PID control for each loop is activated by pressing the "Auto mode" button located near the bottom of the screen else the system will in manual mode by default. The graphs at the bottom indicate the current process variable and their corresponding set-point from the de-coupler. These graphs are important because they indicate the magnitude of the error between the process variable and set-point for each stream.

6 INSTRUMENT CALIBRATION

Instrument calibration is intended to eliminate or reduce bias in an instrument's readings over a range for all continuous values. The purpose of the calibration is "to identify and eliminate any bias in the instrument relative to the defined unit of measurement" (ESH, 2009). Due to the fact that the system was failing to meet the accuracy requirements set by the AS/NZS standard, an instrument calibration check was performed on all the temperature sensors and flow meters to ensure that they weren't responsible for the system's poor performance. Below is a description of the procedures conducted to calibrate the instruments.

6.1 TEMPERATURE SENSORS

The Standard mention Instrument calibration and state that the temperature reading at the inlet of the collector shall be measured to an accuracy of ±0.1°C. They further went on to mention that in order to check that the temperature is not drifting with time, a very much better resolution of the temperature signal to ±0.02°C is required (Standards Australia, 2007)

In the previous years dating back to 2006, Jian conducted a stability test on the temperature sensors to discover if any temperature offsets were occurring between the sensors and to also determine their resolution. The idea was to suspend all the sensors in a container filled with water at ambient temperature by screwing each sensor into a plastic plate that was firmly mounted on the top of the container as shown in figure 10;

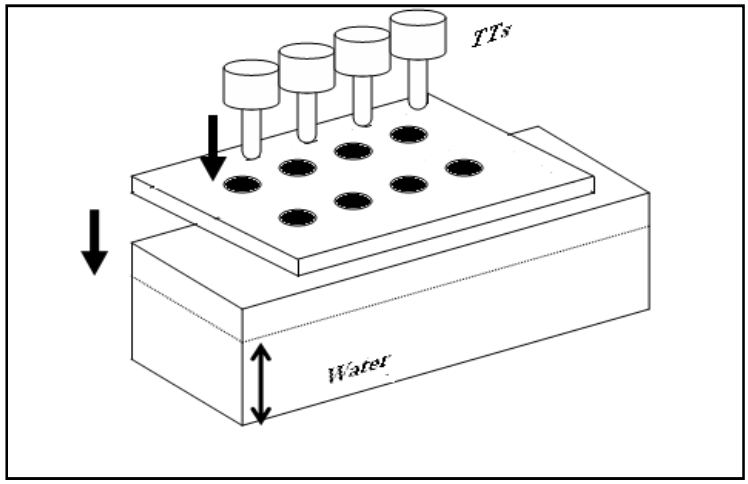

Figure 10: Previous Temperature Transmitter stability test (Mounting)

(Jian, 2006)

The sensors were left in the water overnight while their readings were being continuously logged. This experiment was performed when the extra 3 temperature sensors were available hence a total of 8 signals were recorded. The results were found to be as below;

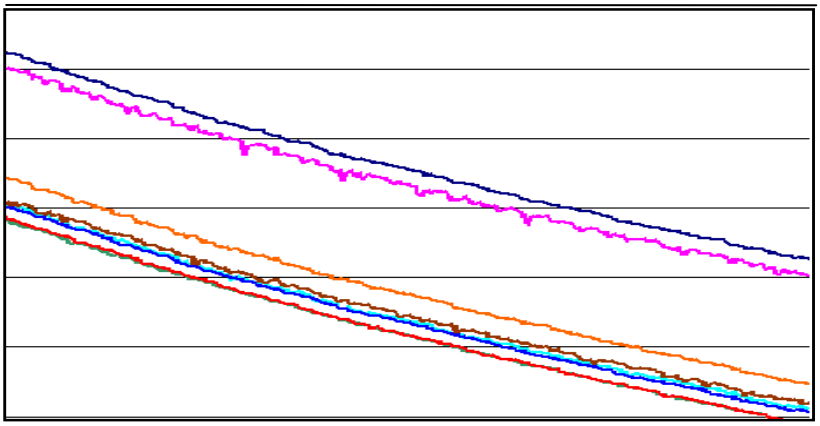

Figure 11: Previous Temperature Transmitter Stability tests (Results)

(Jian, 2006)

The implication conceived from the image above suggested that all the temperature sensors were changing at the same rate but exhibited a minor constant offset from each other. This offset was believed to be present due to different hardware settings in each senor. However, although the sensors were concluded to exhibit an offset from each other, this didn't prove that they were reading the true temperature. Jian then extended his study and empirically demonstrated that the sensors had a 'certificate' accuracy of ±0.15% of the span. The implication made from this result was that sensors had a resolution of ±0.0225°C and failed to comply with the 'very much better resolution of ±0.02°C' as required by the standard.

Nonetheless, this test was performed once again to determine the temperature offsets from one another as instruments change over time. The sensor and container apparatus was difficult to repeat because all the sensors were later sealed onto the system with an adhesive that made the task of dismantling them tricky. Consequently, the alternative test was to run water from the mains supply through the entire system until a steady state temperature for all the sensors was approached. The assumption made for this test was that the temperature of the water coming from the mains supply remained constant. After running water through the system for a few hours, the following sensor steady-states were achieved.

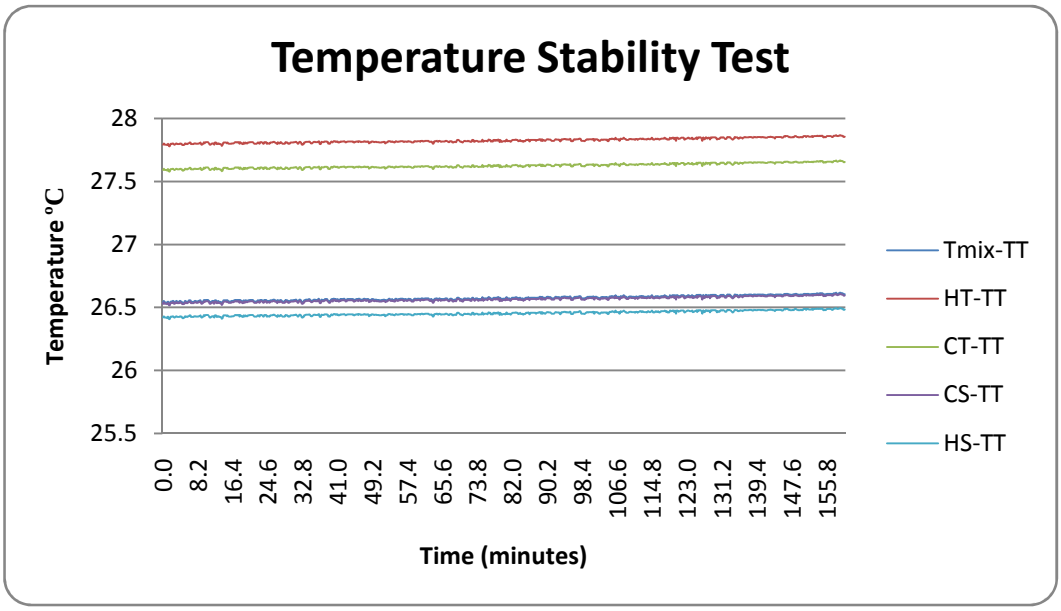

Figure 12: Current Temperature Transmitter Test

The test above shows a steady offset between each of the temperature sensors mounted on the system. The test ran over the duration of approximately 2.5 hours after steady-state values were achieved. A slight raise in water temperature was detected over the duration of the steady state period which suggests an atmospheric raise in temperature caused a heat transfer to the pipes. Jian used the 'Ambient temperature sensor' as the reference temperature and scaled all the other measurements accordingly. However, this sensor was not available through the duration of this project as mentioned previously (pg.30), so the final stream temperature sensor T_{Mix} was used as the reference temperature instead. All sensor signals were then adjusted by small scaling values relative to T_{Mix} in the LabVIEW program. For future purposes, if T_{Mix} was found to have an offset relative to the true temperature, then the user can simply adjust it in the LabVIEW program and not have to worry about adjusting the rest of the signals as they are all relative readings.

6.2 FLOW METERS

According to the AS/NZS standard (Standards Australia, 2007), the accuracy of the liquid flow-rate measurement must be within ± 1.0% of the measured value. Stability tests were conducted on the flow meters to determine their accuracy. A stability test was carried out on the flow meter mounted on the hot water stream. The results below show the steady-state flow-rate for a 9.5 minute period, with a sampling rate of once per second.

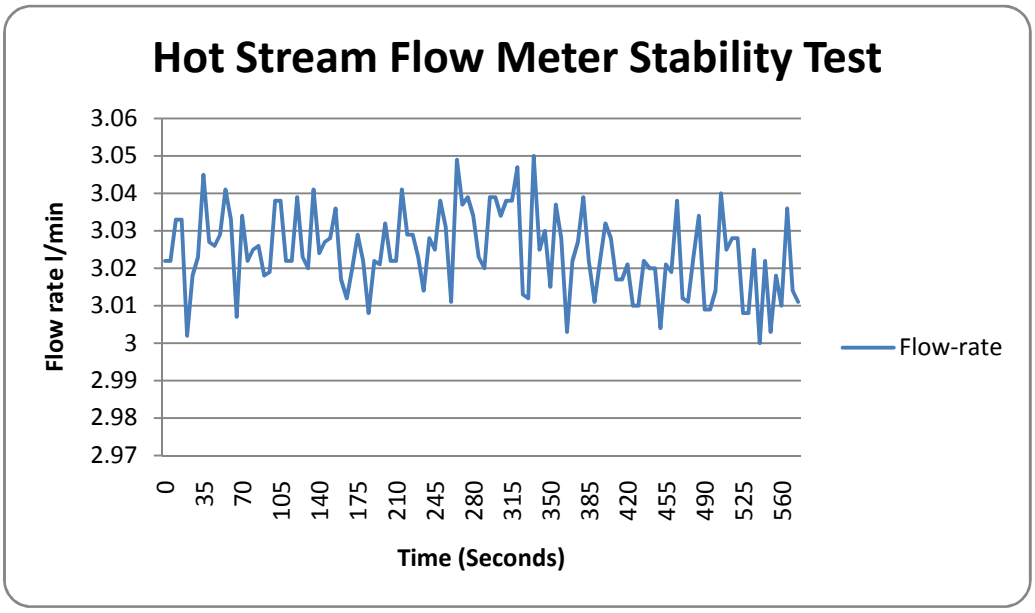

Figure 13: Hot Stream flow meter stability test

The statistical data calculated below reveal the uncertainty of this flow meter measurement

Flow Meter Statistics	
Mean	3.02456
Median	3.023
Standard Deviation	0.011297
Sample Variance	0.08073
Minimum	3
Maximum	3.052
Range	0.052
Maximum Error (l/min)	0.027
Error ±%	0.907

Table 6: Flow Meter Statistics

As mentioned previously, the acceptable flow meter uncertainty given by the standard is ±1% (Standards Australia, 2007). This flow meter appears to have an uncertainty of ±0.907% which implies that flow meter is definitely capable of serving its required task.

7 PROCESS CHARACTERISTICS

7.1 VALVE CHARACTERISATION

Valve characterisation is all about discovering the behaviour of the valves. The characterisation process is intended to test the valves for issues such as linearity and hysteresis. The method by which each valve was characterised was through the use of manual control which allowed each valve to be independently controlled by the user. The results below reveal the properties each valve.

7.1.1 Hot Stream Valve

The hot stream valve was stepped up from 0-100% in 10% intervals and back down again, with the cold stream valve fully closed. The supply feed from the mains was set to 4 l/min as the flow meters cannot read any higher values. The flow-rate response of this stream is shown below

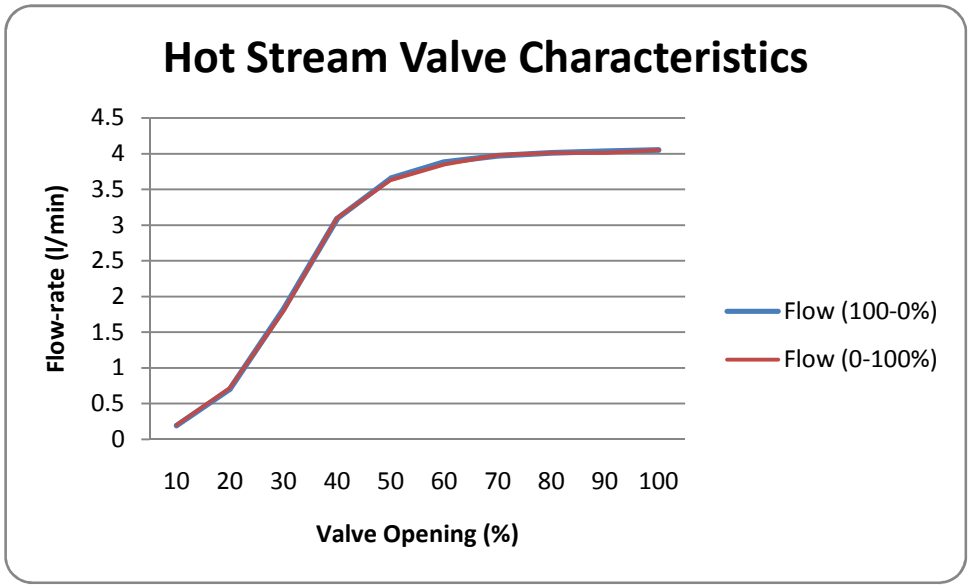

Figure 14: Hot Stream Valve characteristics

The flow response of this valve was not linear for the entire operating range. The flow-rate appears to be linear between the 20-40% valve opening range. No valve hysteresis seemed to be evident from the results above, since both lines are positioned almost identically on top of each other. This implies that the valve returns to a common position no matter where the valve position was previously.

7.1.2 Cold Stream Flow-rate

The same test was conducted on the cold stream flow rate valve, having the valve on the hot stream closed. The valve behaviour for this stream is also shown below;

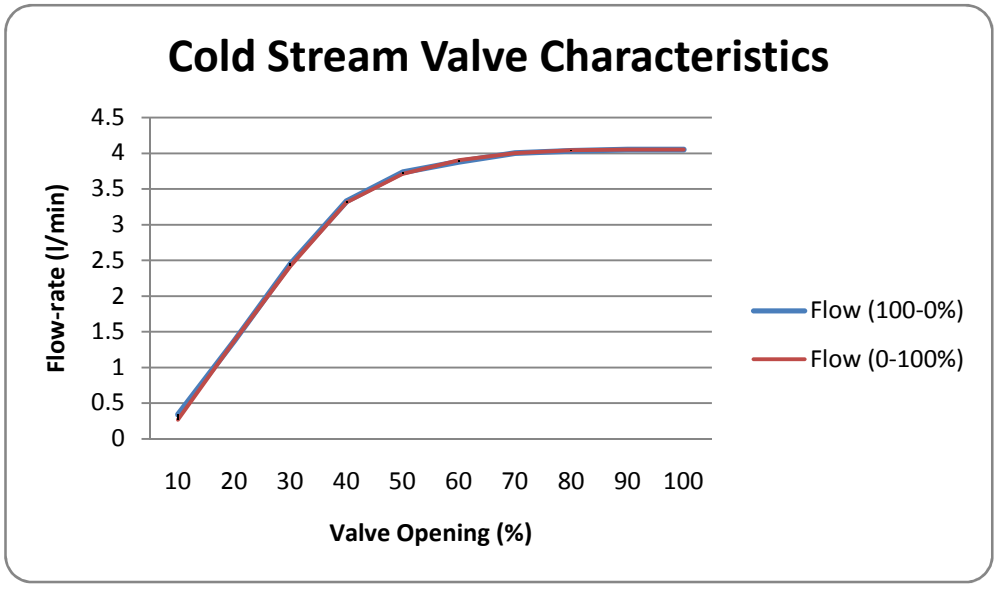

Figure 15: Cold Stream valve characteristics

The flow rate through this stream was proportional to the valve opening percentage for values under 40%. No hysteresis was also evident in the valve, as promised by the manufacturers.

7.2 VALVE STEP TESTS

Several step tests were performed on the valves in manual mode, to acquire their approximate transfer functions. These transfer functions were necessary for the controller loop tuning parameters.

The first step test was performed by initially opening both control valves to 20% then stepping the cold stream control by a magnitude of +10% the response is shown below;

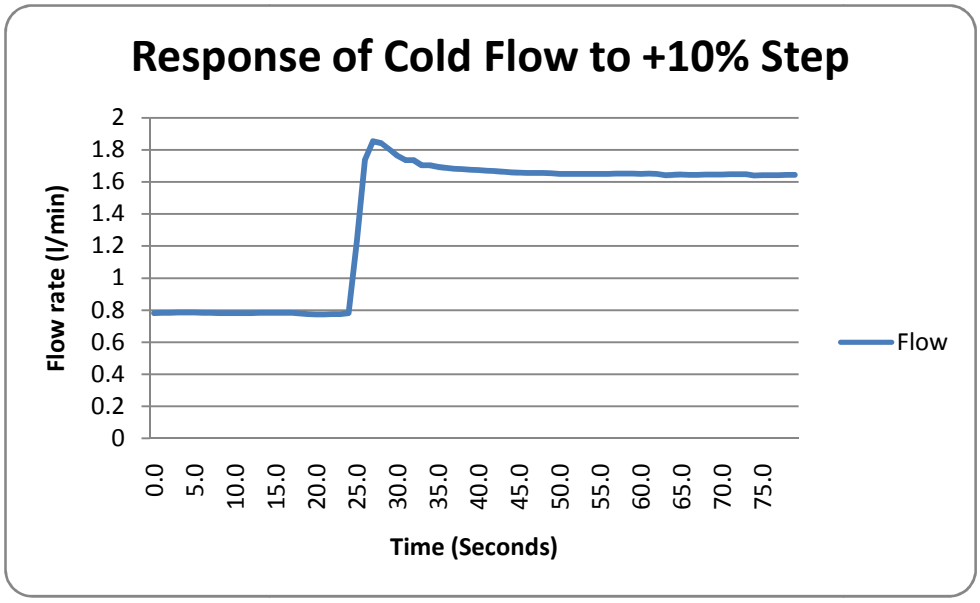

Figure 16: Response of cold flow to +10% step change

Upon a 10% step change, the cold stream flow-rate rapidly increases and overshoots by a small amount before it settles to a steady-state. The overshoot occurs due to the flow-rate interaction between this stream and the hot flow stream. Furthermore, after a step change was requested at 25 seconds, no time delay was noticeable from the response which suggests that the valve reacts quite fast upon receiving the signal.

Below is the response of hot stream flow rate as a consequence to the step change made on the cold stream.

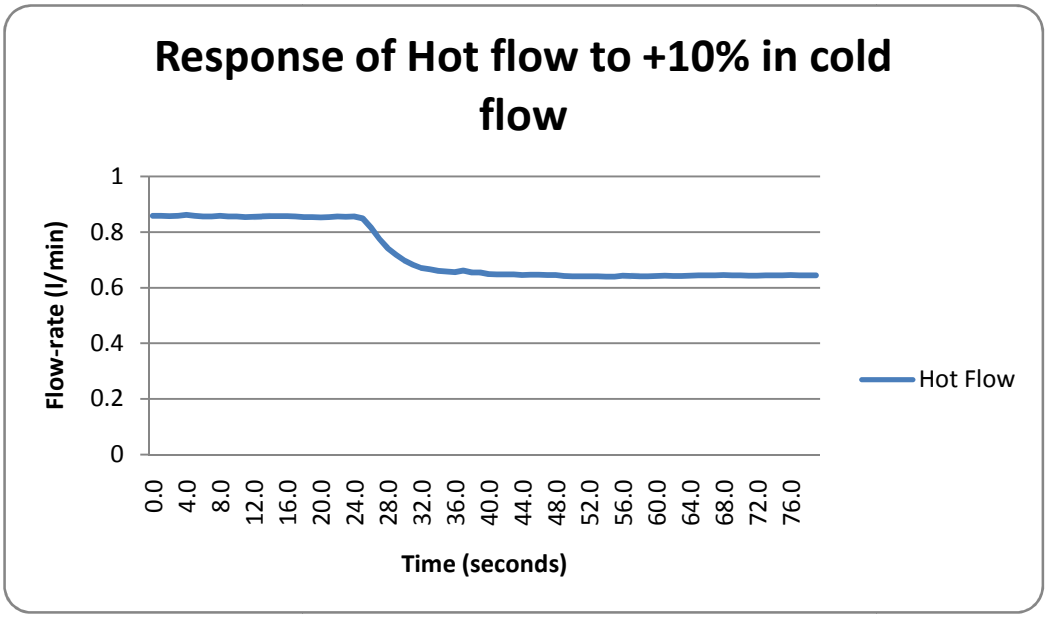

Figure 17: Response of hot flow to +10% in cold flow

A flow rate interaction occurs because both the hot and cold water tanks are connected to the same supply feed which means the supply pressure gets divided between these two tanks. When the cold stream flow valve is stepped, a bigger supply pressure is sent to the direction of cold water tank to compensate for the increase in outflow. This pressure variation consequently forces a lower supply pressure to the hot tank which immediately results in a first order decrease in outflow as shown in the response above. It is interesting to note that the magnitude of the negative gain on the hot stream is equivalent to the magnitude of overshoot seen in the response of the cold stream flow rate.

The second test performed was identical to the first test above, but this time, the hot stream valve was stepped by a magnitude of +10%. The responses for this test are shown below;

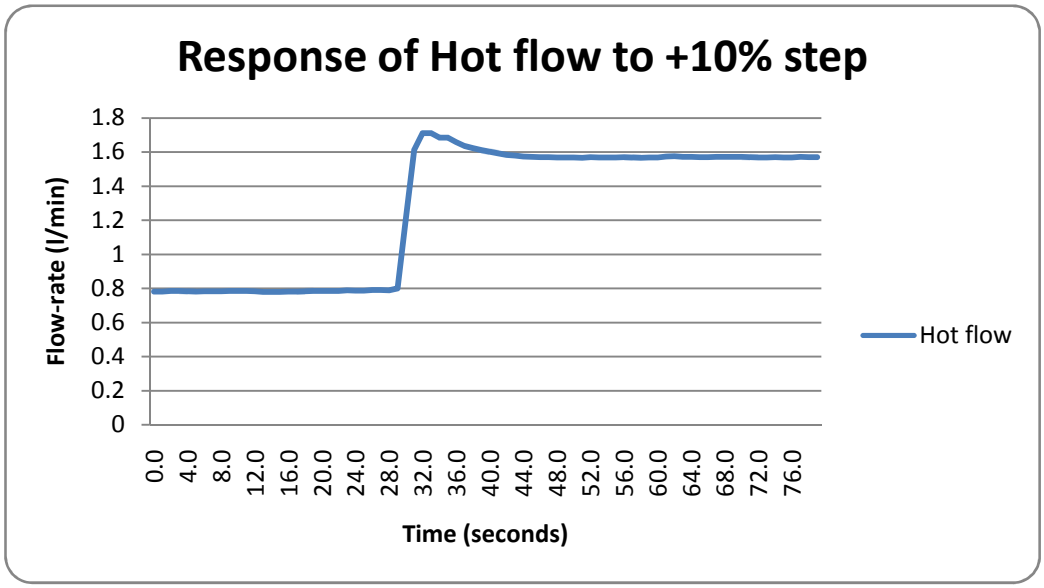

Figure 18: Response of hot flow to +10% Step change

The flow-rate response of this step test was very similar in behaviour to the cold stream flow rate seen above with both developing a gain of 0.8 l/min. The overshoot of this response is slightly smaller in comparison with the cold stream response.

A response of how the cold stream flow responded to the step change performed on the hot stream is shown below;

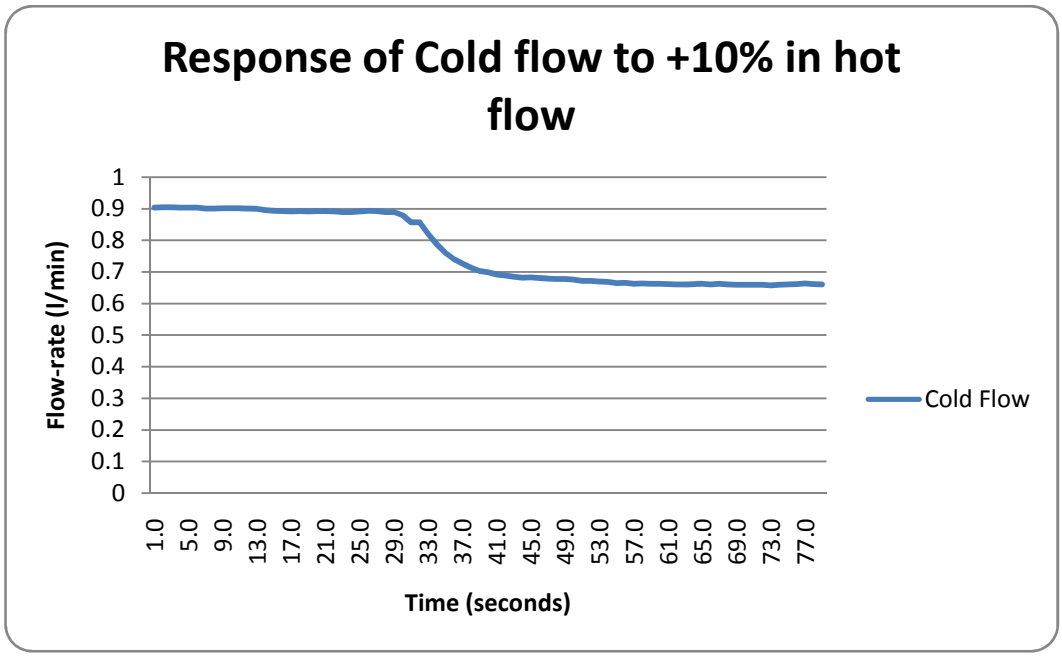

Figure 19: Response of cold flow to +10% Step change in hot flow

The cold flow decreases in a first order form. The gain is also approximately the same as the cold flow response in the first step test.

Several more tests have been performed within the linear regions of the valves to characterise their behaviour. The findings were that both valves always had fairly similar responses in terms of process gain and response type. These results then gave enough evidence to conclude that both valves shared a common transfer function

7.3 TUNING PARAMETERS

The responses above were modelled by a first order transfer function with a time delay using the process reaction curve (Ogunnaike, 1994 pg.535). The derived transfer function was then deduced to be:

$$G(s) = \frac{0.8e^{0.5s}}{1.9s + 1}$$

Equation 9: Valve Transfer function

Hence, by using the Ziegler Nichols approximate PID Tuning Rules [App.C], the following PI parameters were calculated;

$$K_C = 1.125, T_i = 0.028$$

A theoretical model of the system was implemented in SIMULINK to provide a basic indication of how the flow rates would respond to the control parameters above.

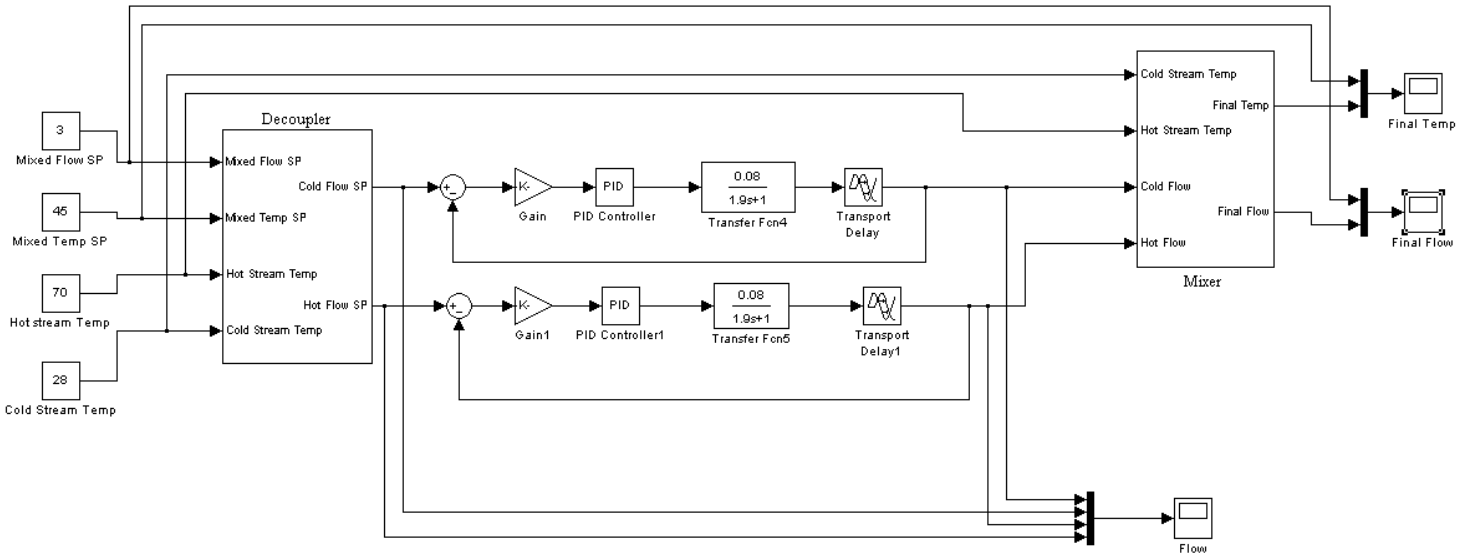

Figure 20: Simulink Block diagram

The de-coupler above calculates flow set-point for each stream under these following assumptions;

- Final Flow-rate set-point = 3 l/min
- Final Mixed Temperature set-point = 45°C
- Hot Stream temperature = 70°C
- Cold Stream Temperature = 28°C (Ambient)
- No heat loss occurs in the pipes between temperature transmitters mounted before the valves and the final stream temperature transmitter -T_{Mix}

Figure 21 shows a theoretical representation of how both streams are to approach their set-point.

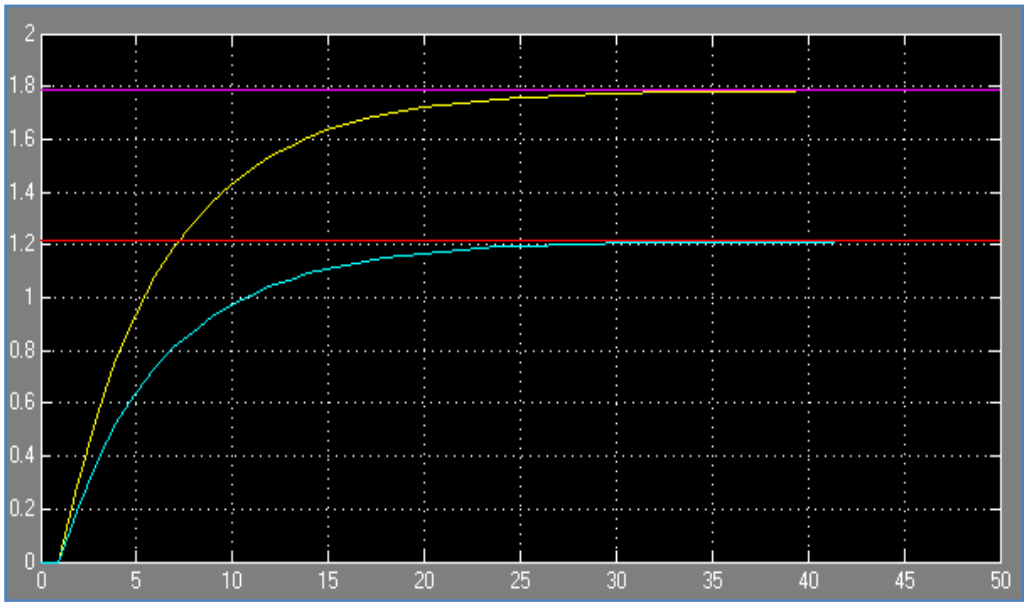

Figure 21: Theoretical set-point Simulation in SIMULINK

The graph above shows that with the approximate PI tuning parameters calculated for each controller loop, the flow-rates should theoretically approach the set-points issued by the de-coupler in first order form. This response is modelled with both valves closed as the initial condition and also assumes that no noise exists in the flow-rate signal

A simulation of how the final flow-rate of the system is approached is represented in the theoretical Simulink response below in figure 22.

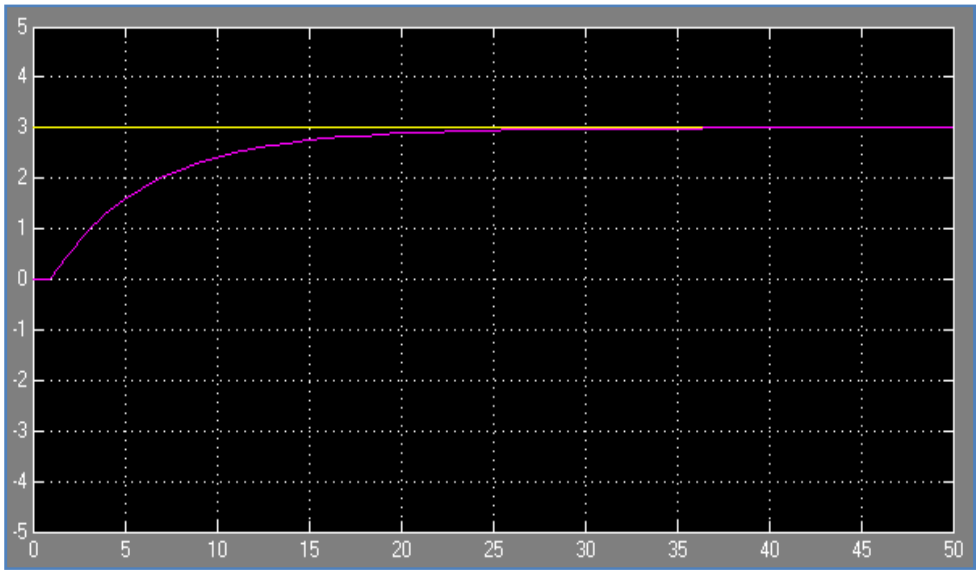

Figure 22: Theoretical final-flow simulation in Simulink

This response indicates that the product of both streams will reach a flow-rate of 3 l/min also in first order form.

In general, the simulated responses provided above are only intended to demonstrate the form of how the flow-rates should theoretically reach their set-points with the calculated PI parameters. The system's set-point response time is not of real interest in regards to how the overall system's performance is measured. However, the main aim of this project is to get the system to abide by the accuracy constraints of the standard once the system reaches a steady-state.

8 PROJECT ADJUSTMENTS

8.1 TEMPERATURE OFFSET

Running the system with the old control scheme was sustained with the new valves installed. Set-point tests were immediately carried out on the system and it was realised that the final stream temperature always had some sort of offset from its desired set-point. This offset was also evident in the mean values of the results developed by Al-Senaid, but was left untreated. Figure 23 shows the apparent offset of a test conducted to further clarify this issue.

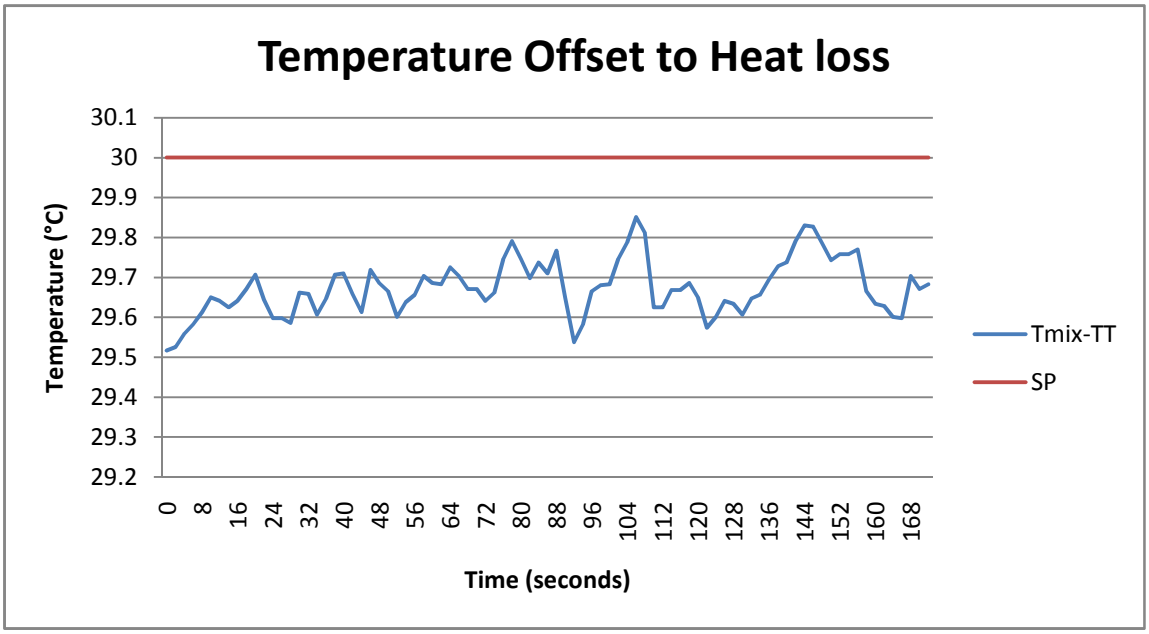

Figure 23: Temperature offset before

After the Flow-rate set-points were reached by each stream, the theoretical temperature of the mixed stream should have been at 30°C. However, a slight temperature offset of about -0.2° occurred and it was believed to be due to heat loss in the pipe after the hot stream temperature sensor as demonstrated by the red line, previously in figure 4.

A test was conducted to verify the magnitude of the heat loss due to pipe radiation between the hot stream temperature transmitter (HS-TT) and the final mixed stream temperature transmitter (T_{Mix} – TT).

At the time of the test, the hot water tank temperature was hovering at steady-state temperature of 73.5°C. At this steady-state, both temperature sensor readings were logged with a hot stream flow-rate of 2 l/min. The results of this test are illustrated in figure 24;

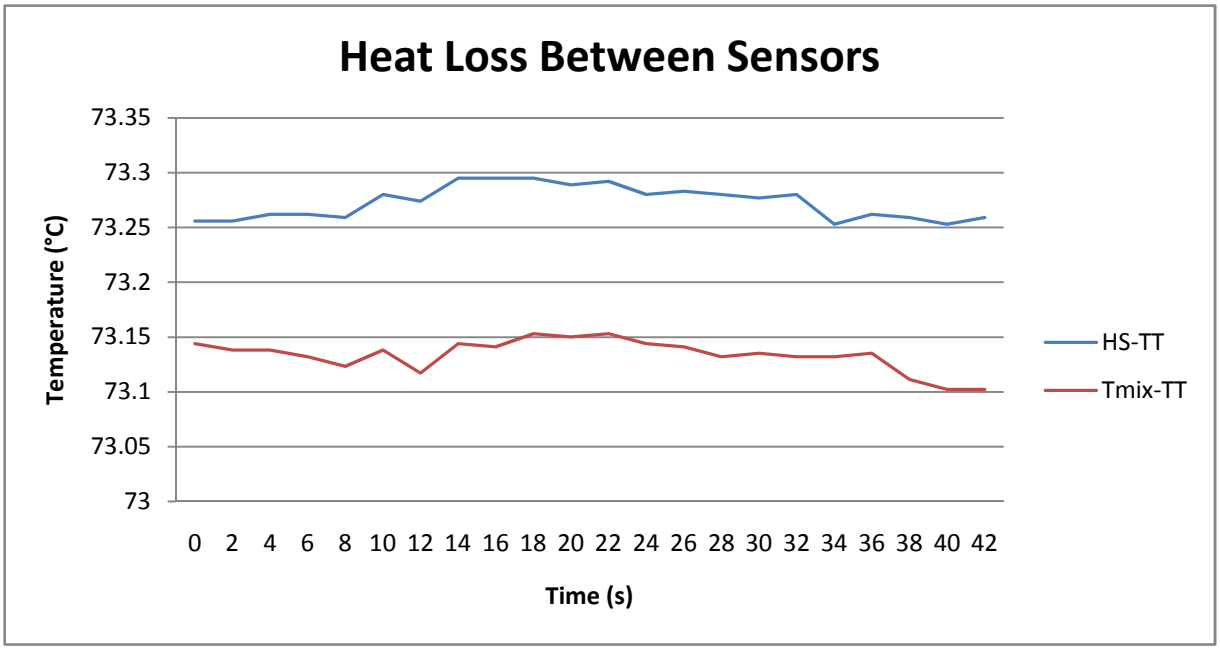

Figure 24: Heat loss between transmitter readings

By the time the flow from the hot water tank reached the hot stream temperature transmitter, an approximate 0.22°C decrease in flow temperature occurred. The pipe running from the outlet of the tank was well insulated but was interfaced with another pipe that provided partial insulation by an integrated material in the pipes dynamics. Assuming the temperature transmitters were calibrated correctly, the heat radiation through this pipe was responsible for the 0.22°C heat loss at that point. By the time the water reached the last temperature transmitter T_{Mix}, the temperature was detected to be approximately 0.12°C less than what it was back at the hot stream temperature transmitter. The T_{Mix} transmitter is mounted on a connecting copper pipe which also was not insulated. The product of the final heat-loss through the pipes accumulated to be approximately 0.34°C which is evident in the offset seen in Figure 23.

The purpose of the additional PI control loop was to eliminate the final temperature offset by opening the hot stream valve by a small percentage and consequently closing the cold stream valve by the same magnitude to keep the final flow-rate constant. This was achieved by adding the output of the PI controller with the set-point issued by the de-coupler.

After the implementation of the PI control loop, another test was conducted under the same conditions to verify if the offset had been eliminated. Figure 25 reveals the result.

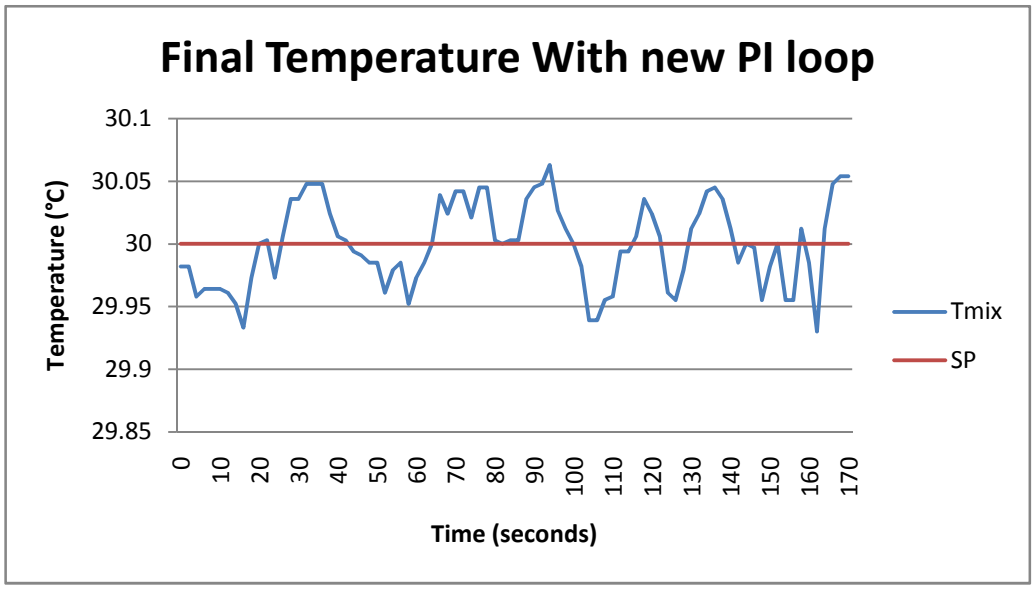

Figure 25: Final Temperature with offset elimination

The figure above indicates that the PI controller has forced the offset to be eliminated by simply adjusting the flow-rate of each stream.

8.2 LOOP TIME

The LabVIEW loop was considered to be a suspicious factor which was affecting the performance of the system. The program loop time was initially set to 500ms when the Baumann valves were being used, however this time did not necessarily need to apply with the new valves since they had a rapid reaction time. Several tests were carried and logged to examine the system's performance while running under various loop times. Table 8 shows how the system performed as a measure of standard deviation with the corresponding loop times.

Loop Time (ms)	FLOW STDEV	TEMP STDEV
1000	0.0219	0.089
500	0.017	0.061
300	0.014	0.058
250	0.013	0.045
220	0.014	0.047
200	0.016	0.059

Table 7: Loop Time Performance

The table above suggests that when the loop time of 250ms was set, the standard deviations of the process variables were at best. Any loop time smaller than 250ms was handled by the PC; however the loop time became unstable upon logging the data. The smallest loop time achievable by the PC was 167ms if a value of 0 was assigned to the loop time.

8.3 HOT WATER TANK CONTROL

The AS/NZS standard recommended conducting a solar collector efficiency test with an inlet temperature of 70°C at a flow-rate of 3 l/min. This recommendation implies that the temperature in the hot water tank must be able to maintain temperatures of over 70°C with a 3 l/min output. Since the input temperature of the water is supplied at an ambient temperature from the mains, the issue of concern is whether the heater is able to sustain water temperatures of 70°C or above when there is an inlet flow-rate of 3 l/min at ambient temperature.

Suppose water was entering the tank at an ambient temperature of 28°C, the question of interest is how much energy is required to heat the water to a temperature of 70°C,
with an input flow-rate of 3 l/min?

The calculation below indicates how much energy is required to heat the water and how long it would take the heater, when it is operating at maximum power (14400W) to raise the input temperature of the water to 70°C.

Using the equation;

$$Q = MC_P(T - T_i)$$

Equation 10: Energy balance

Where;

Q = Energy lost or gained

M = Mass

C_P = Heat Capacity

T = Final temperature

T_i = Initial temperature

The heat capacity of water is 4.184 J ml^{-1} C^{-1}

Hence, the amount of energy required to heat 3 litres of water from 28ºC to 70°C is;

$$Q = 3000 * 4.184(70 - 28) = 527184\,J$$

Equation 11: Energy required to heat water from 28º-70°

The time it would take the heater to theoretically heat the water can be calculated by the equation;

$$P = \frac{E}{T}$$

Equation 12: Power equation

Where;

P = Power (W)

E = Energy (J)

T = Time (S)

By rearranging the equation as a function of time, the time required would be;

$$T = \frac{527184}{14400} = 36.61\ seconds$$

Equation 13: Time required to heat water

The calculation from Equation 13 suggests that the heater is able to heat the input water to 70°C before the same amount of water leaves the tank (1 minute). So in theory, the heater is capable of keeping the water at 70°C and above, after the effect of the input temperature disturbance has passed away. On the other hand, the input ambient temperature is also subject to vary, especially in the winter season where water temperatures from the mains supply can become substantially lower than the atmosphere temperature. In consequence, this would further present an additional threat to the heating element as it must exert extra energy over a shorter period of time to raise the temperatures of the rather cooler inlet feeds to the 70°C set-point. By this account, it is definitely worth calculating what the minimum feasible inlet temperature could possibly be, if the heater is to succeed. By re-arranging equation 12 as a function of energy, the heater is theoretically capable of supplying 864000 Joules of energy per minute. By substituting this value for "Q" in equation 10 and solving for T_i, the minimum feasible inlet temperature that the heater would be able to handle calculates to be 1.16°C. This is of course under the assumption that the heat energy gets evenly distributed over the entire volume of the tank, and that the heater is in fact operating at the full rated power.

A test was conducted to verify if the water in the tank could maintain temperatures of 70°C or above with an outflow of 3 l/ min. The graph below in figure 26 shows how the temperature in the hot water tank varied, after initially heating the water to a maximum temperature of 78°C, and subsequently allowing an inlet flow-rate of 3 l/min at ambient temperature of 28°C as a disturbance.

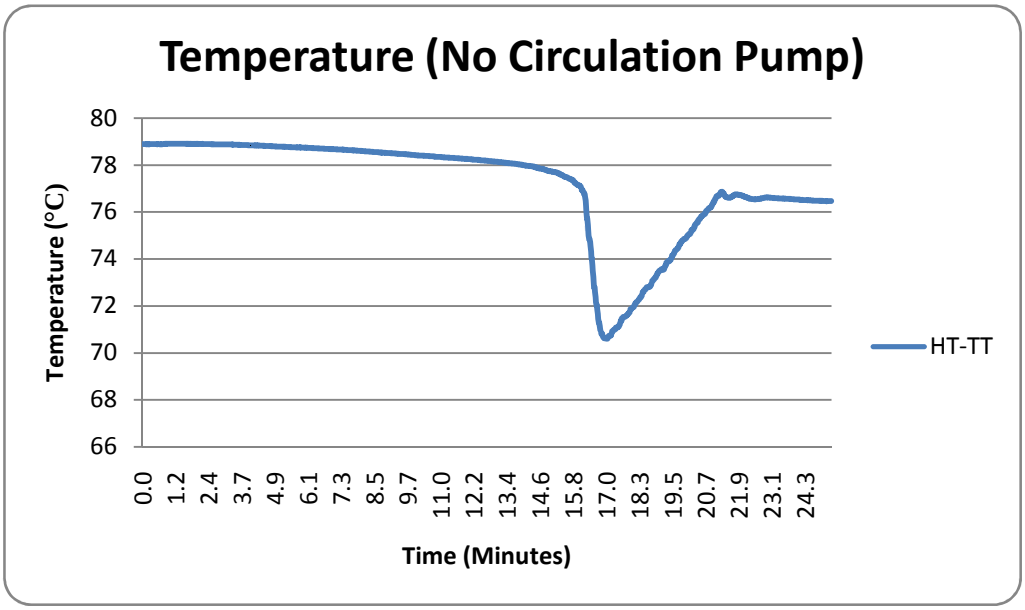

Figure 26: Hot water tank temperature with no Circulation Pump)

The temperature response in figure 26 represents the worst case of temperature deviation in the hot water tank when it is subjected to the largest energy disturbance in terms of input flow-rate. After approximately 3 minutes, a minor steady temperature decrease is detected by the HT-TT as a result of the disturbance. After approximately 15 minutes, the temperature at that stage had only dropped by 0.8°C followed by an unexpected sudden dip in temperature one minute later for no theoretical reason. Therefore, although the heater in the tank was able to handle the disturbance for the required time without the use of the recycle pump, the physical response of figure 26 contradicted the implication made by theoretical viewpoint which suggested a total disturbance rejection. For this reason, it may become questionable whether the heating elements were in fact activated at full power for the duration of the test. Hence, further future consideration is required in regards to this issue to justify the rather bizarre nature of this response.

The purpose of the recycle pump is to grant a more uniform temperature gradient within the tank. A test was also conducted to examine how the temperature responded to the same disturbance but with the pump operating at its highest speed.
The result of this test is shown below in figure 27;

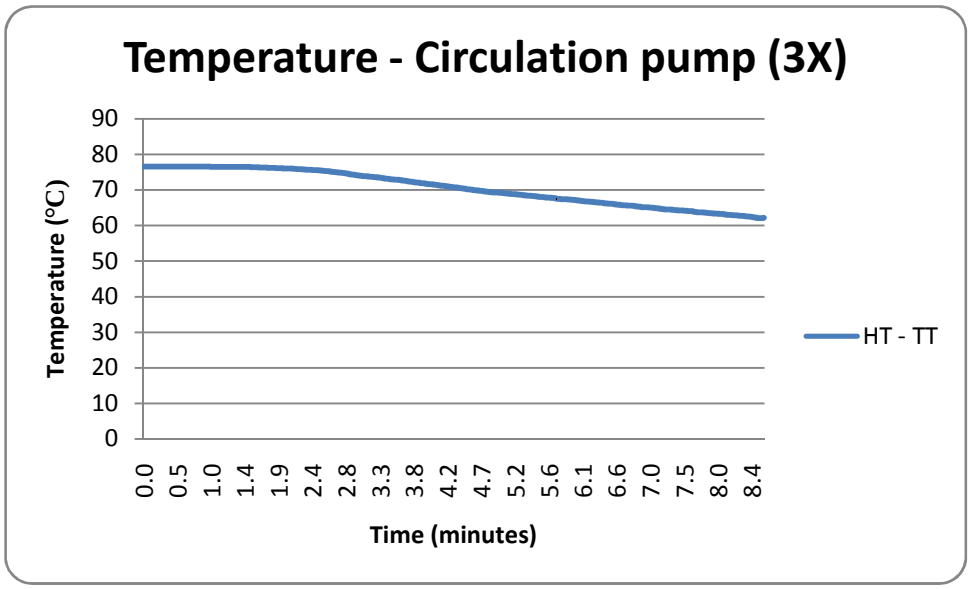

Figure 27: Hot water tank temperature with circulation pump x3

Activating the circulation pump helps the temperature distribution in the tank to become uniform at a much faster rate than when it is switched off. This is achieved by constantly circulating hot water from the outlet of the tank to the combine with the cooler water entering through the inlet. Approximately two minutes after the application of the disturbance, a

temperature decrease was detected by the HT – TT and consequently linearly decreased at a much faster rate than when the pump was not on duty. Five minutes later, the temperature passed the 70°C mark and continued to steadily decrease. It was found that having the pump turned on did not allow the heater enough time to concentrate its energy on a specific volume of water, but rather add its heat over multiple stages as the flow was constantly being circulated. Therefore, the implication of having the circulation pump switched on will cause the effect of the disturbance to occur much faster than if the pump simply was not activated. Since the effect of the disturbance can be evidently avoided for the required 15 minute period of a steady-state test as seen in figure 26, activating the circulatory pump only introduces disadvantages to the scenario in this case.

The tests above were both conducted with the heater set to maximum power. This implies that the PID control loop around the heater is found to be superfluous because the heater should be set to maximum power at all times to assure the water temperature in the tank never drops below 70℃.

9 RESULTS

9.1 VALVE PERFORMANCE COMPARISON

After the implementation of the new valves, some steady-state tests were performed to compare the steady-state performance of the system with the new proportional control valves, in contrast to the previous performance of the system with the old Baumann pneumatic valves. A comparison test was performed while keeping the final flow-rate constant at 3 l/min.

The first performance comparison is shown below for a set-point temperature of 30℃ in the steady-state final flow;

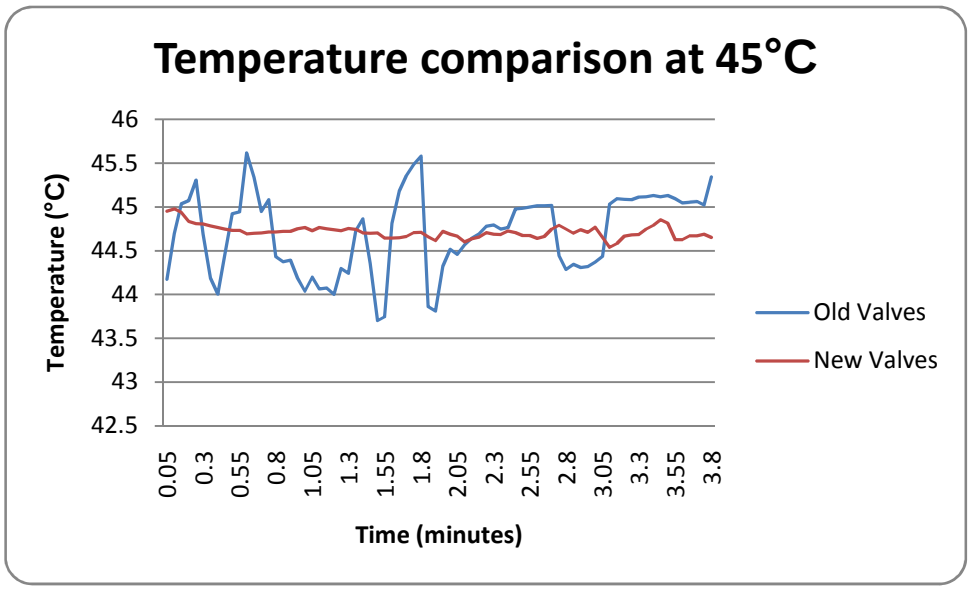

Figure 28: Temperature comparison at a 45°C steady-state

An instant improvement in the steady-state performance of the system is seen in reaction to the new valves. The temperature offset observed above was prior to the implementation of the additional PI controller. Just by observing these signals, it can be definitely confirmed that the system's performance dramatically improved when the hysteresis factor was eliminated from the equation. The abrupt temperature fluctuations that occurred by the use of the old valves, are a strong reflection of the flow-rate control havoc that once existed. The flow-rate performances shown on the next page will further clarify this point.

Below in figure 29, are the corresponding final flow-rate responses in terms of each valve type;

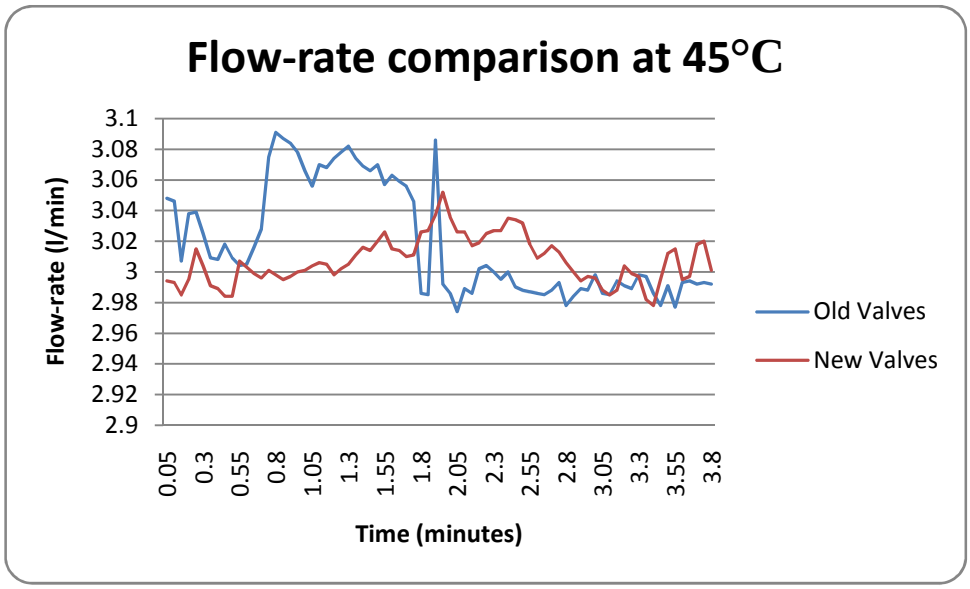

Figure 29: Flow-rate comparison at a 45°C steady-state

The steady-state response of the final flow-rate under the influence of the old valves is quite poor in comparison to the steady-state achieved with the new valves. It comes as no surprise to see large fluctuations in the final temperature after viewing the flow-rate response of the old valves. The hysteresis present in these valves certainly provoked aggressive control judgements on the individual streams. Justification for the responses above is shown on the next page, of how each flow-rate was controlled by the competing valves.

Steady-state response of the hot stream flow-rate under the effect of each valve;

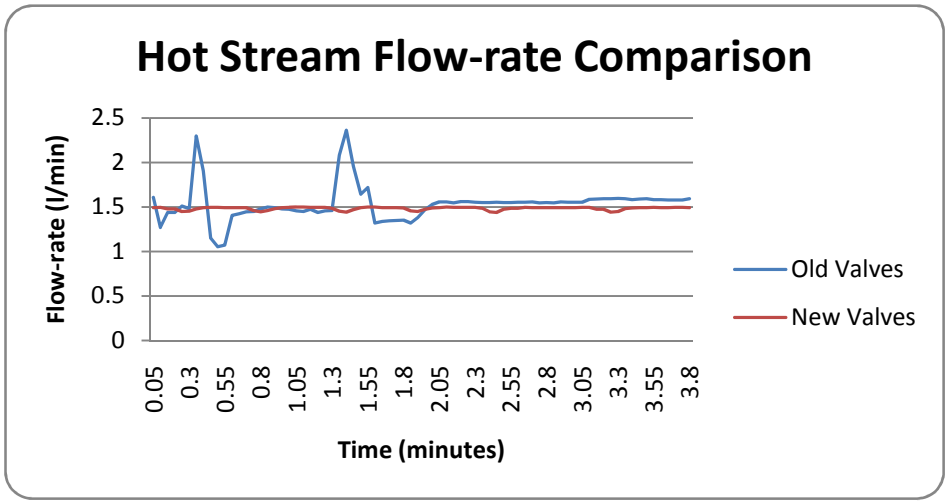

Figure 30: Hot stream steady-state performance comparison

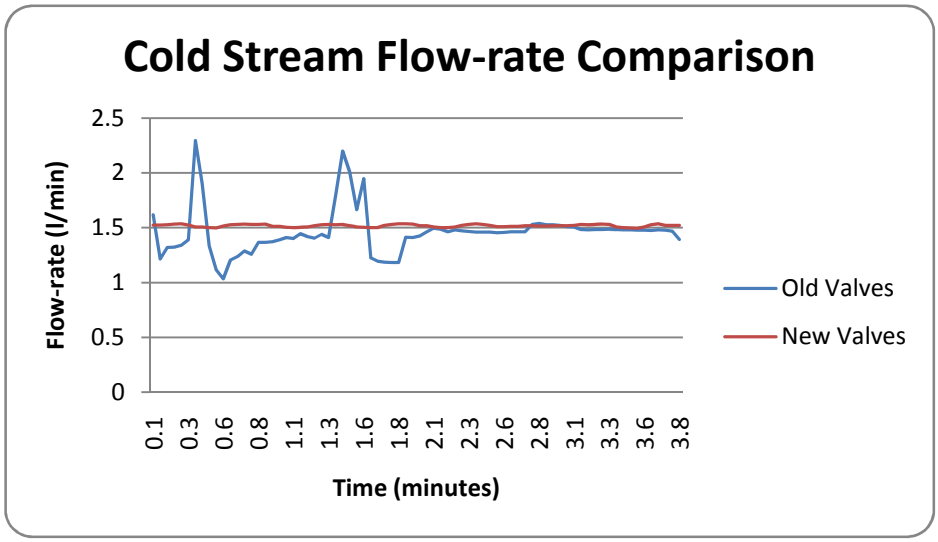

Figure 31: Cold stream steady-state performance comparison

The abrupt changes in the flow-rates of the hot and cold streams when controlled by the Baumann valves, suggests that the effect of the hysteresis was quite detrimental to the overall performance of the system. When the a control command was sent to each valve to slightly open the valve positions to where they should be, the force build up on the stems eventually overcame the resistance of the 'stickiness' in those positions, but consequently generated an abrupt overshoot in valve position which caused an unnecessary sudden increase in flow-rate. On the other hand, since the new motor driven control valves were quoted and proven not to exhibit any hysteresis, there would be no theoretical reason for such spikes to occur from the perspective of the valves.

9.2 TEST PROCEDURE

The AS/NZS standard declare that the efficiency testing procedure should consist of at least four inlet fluid temperatures that are spaced evenly over the operating temperature range of the collector. The standard also states that the time frame for each test shall be for a 15 minute period, after the steady-state values of the correct fluid measurement temperatures are achieved.

9.3 ACHIEVING SYSTEM STEADY-STATE

There was some ambiguity in the worded structure of the text to clarify the conditions of which the system must satisfy to determine if a valid steady-state exists. The standard states;

Part 1:

"A collector is considered to have been operating in steady-state conditions over a given measurement period if none of the experimental parameters deviate from their mean values over the measurement period by more than the limits given in table 1."

Part 2:

"To establish that a steady-state exists, average values of each parameter taken over successive periods of 30 seconds shall be compared with the mean value over the measurement period."

(Standards Australia, 2007)

Table 1 – Permitted deviation of the measured parameters during a measurement period

Parameter	Permitted deviation from the mean value
Test solar irradiance	± 50W/m^2
Surrounding air temperature	± 1 K
Fluid mass flow-rate	± 1%
Fluid temperature at collector inlet	± 0.1 K

Figure 32: Conditions of Steady-state by standard

(Standards Australia, 2007)

The way by which the system is perceived to have established a steady-state without violating any of the constraints given in the table above, is quite a controversial matter.
There are two apparent interpretations that are drawn from the written text, for how the system should be tested to determine if a steady-state exists.

9.3.1 First interpretation of Steady-state

The first interpretation implies that a system is considered to be in an operational steady-state if;

Under no circumstance shall the process variables violate the bounds given in table 1 for the duration of the test.

The logic behind this interpretation is formed by the assumption that Part 1 of the text is a condition of its own that must be satisfied independent of what is written in part 2.

9.3.2 Second interpretation of steady-state

The second interpretation implies that a system is considered to be in an operational steady-state if;

The average value of each process variable taken over successive periods of 30 seconds never violate the bounds in table 1 after they have been compared with the mean value of the measurement in the entire 15 min period.

Conversely, the reasoning behind this interpretation is formed by the assumption that 'part 2' is a clarification to how part 1 should be determined, under the assumption that part 1 is not an independent condition.

The insinuation of the first interpretation proposes that the process variables are to be measured as absolute values within the constraints. If this interpretation is what is truly implied by the standard, then the system must perform under more strict conditions in comparison with the acceptable performance of the system by the second interpretation.

Three steady-state tests were conducted on the system to verify if the performance proved to satisfy the accuracy criteria provided by the standard. The results of the steady-states were evaluated by each interpretation to determine if the system's performance qualifies to test a solar collector's efficiency.

9.4 STEADY-STATE PERFORMANCE

9.4.1 Steady-state at 30℃

The first test conducted was to configure the system to provide a fluid inlet temperature of 30℃ at 3 l/min. This temperature was selected to correspond with one of the inlet temperatures quoted by the standard. A 15 minute steady-state test was recorded with a sample rate of once per second, to assess the system's performance. The results of this test are graphically and statistically shown below in terms of both temperature and flow-rate;

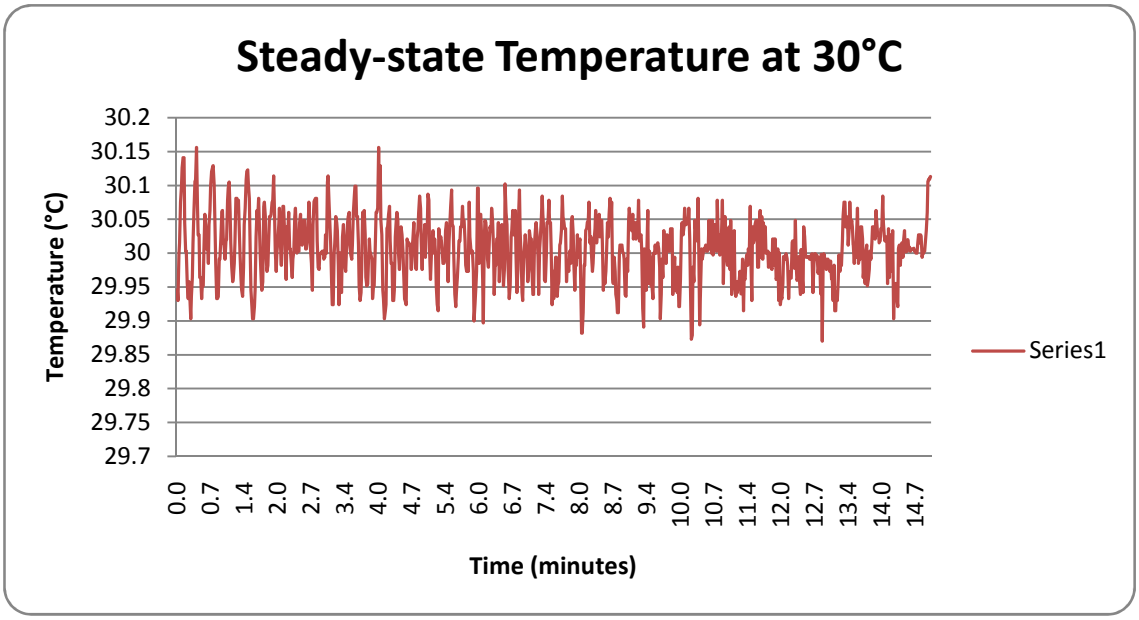

Figure 33: Steady-state Temperature at 30℃

Steady-state Temperature – 30°C	
Mean	30.0032
Median	30.006
Standard Deviation	0.046
Maximum	30.156
Minimum	29.87
Range	0.28
Error ± (°C)	0.156

Table 8: Statistical data for steady-state temperature of 30℃

The system's temperature steady-state performance was to be evaluated by 'interpretation one', then this parameter instantly violated the ±0.1℃ deviation from the mean as seen in the graph above although most of the values were within the acceptable bounds. Hence the temperature steady-state performance is considered to have broken the rules.

Evaluating the system's steady-state operation under 'interpretation two' involves averaging samples over successive 30 second periods and comparing them with the mean of the entire measurement (30.0032). The results for this procedure are shown below.

Sample	1	2	3	4	5	6	7	8	9	10
Mean	30.018	30.019	30.033	30.009	30.020	30.020	30.011	30.009	30.014	30.009
Error (°C)	-0.015	-0.016	-0.030	-0.006	-0.017	-0.007	-0.008	0.006	-0.011	-0.006

Sample	11	12	13	14	15	16	17	18	19	20
Mean	30.013	29.999	30.016	30.006	30.009	29.999	30.007	29.991	30.008	29.990
Error (°C)	-0.010	0.004	-0.013	-0.002	-0.006	0.005	-0.004	0.012	-0.005	0.014

Sample	21	22	23	24	25	26	27	28	29	30
Mean	29.998	30.019	29.981	30.006	29.980	29.985	30.000	30.010	29.999	30.024
Error (°C)	0.005	-0.016	0.022	-0.003	0.023	0.018	0.003	-0.007	0.004	-0.020

Table 9: Steady-state Temperature errors at 30℃

After comparing the mean of each sample with the average of the entire sample, it is evident by the error readings above to see that the system has achieved a steady-state with none of the sample averages deviating from 30.0022 by ±0.1°C. Therefore by this interpretation of the standard, the system has proved to be well within the ±0.1℃ accuracy criterion and thus qualifies by the standard as an acceptable steady-state performance.

The steady-state analysis in terms of the flow-rate parameter of this test is illustrated in figure 34 below;

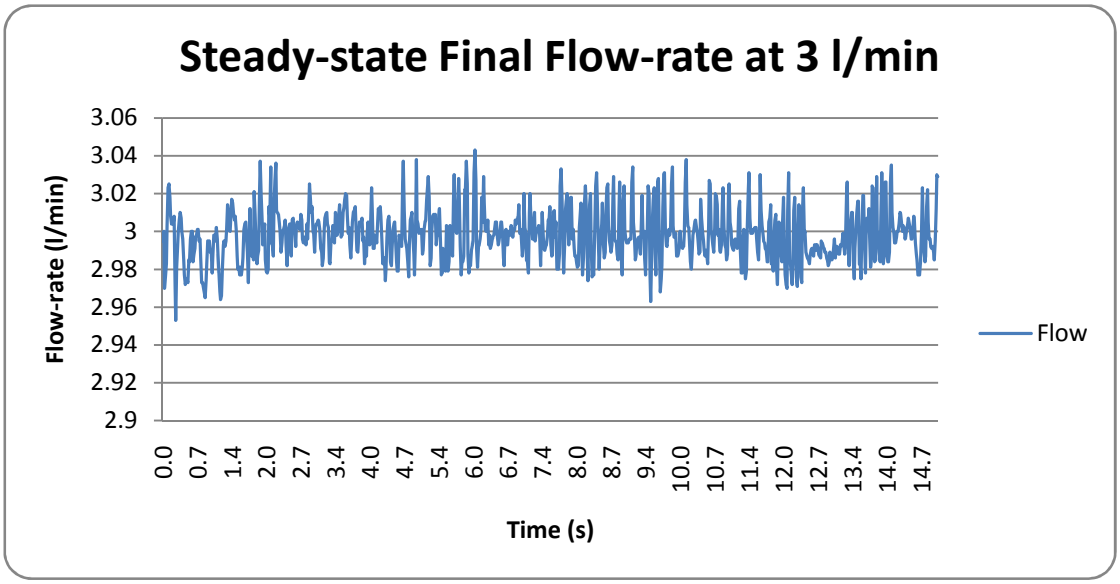

Figure 34: Steady-state Flow-rate for a 30℃ inlet temperature

Steady-state Flow-rate at 30°C	
Mean	2.998
Median	2.997
Standard Deviation	0.014
Maximum	3.043
Minimum	2.953
Range	0.09
Error ± (l/min)	0.045

Table 10: Statistical data for steady-state flow-rate at 30℃

The acceptable deviation from the mean for this parameter is quoted to be within ±1% of the mean value. This means that for a flow-rate of 3 l/min, all of the steady-state values of the flow-rate must be within the range of ± 0.03 l/min of the mean. Once again, this bound has been violated by 'interpretation one' of the standard, as the error bound in the table above for this parameter was measured to be ± 0.045 l/min. Hence the system is not performing to an acceptable steady-state condition. Furthermore, even if this parameter was hypothetically found to be within ±0.03 l/min, the system steady-state for this test would still not be considered eligible to test a solar collector because all the steady-state parameters have to satisfy their corresponding restrictions and this has already been broken by the temperature parameter.

On the contrary, if the flow-rate performance was to be tested for eligibility by 'interpretation two' of the standard, then the results of the table below would once again need to be analysed to approve if valid steady-state exists

Sample	1	2	3	4	5	6	7	8	9	10
Mean	2.993	2.987	2.994	2.996	3.000	3.002	3.000	3.002	2.998	2.999
Error (l/min)	0.005	0.011	0.004	0.002	-0.002	-0.004	-0.002	-0.004	0.000	0.000

Sample	11	12	13	14	15	16	17	18	19	20
Mean	2.999	3.000	3.003	2.999	2.999	3.001	2.998	3.001	2.999	3.001
Error (l/min)	-0.001	-0.002	-0.005	-0.001	-0.001	-0.002	0.001	-0.003	0.000	-0.003

Sample	21	22	23	24	25	26	27	28	29	30
Mean	2.999	3.002	2.997	2.996	2.993	2.989	2.996	3.001	3.002	2.998
Error (l/min)	-0.001	-0.004	0.001	0.002	0.005	0.009	0.002	-0.003	-0.004	0.001

Table 11: Steady-state flow-rate errors at 30°

By examining the errors of each sample in reference to the ultimate mean, this steady-state parameter has comfortably remained within the quoted bounds of ±1%.

Due to the confusion of how the system's steady-state performance should be determined, to comply by the standard, by regulation the system must be tested in reference to the 'worst case scenario' as a precautionary factor. Therefore, the performance must be assessed by the means of 'interpretation one', since the system is expected to perform at a higher level to satisfy the constraints.

In consequence to the matter above, since the performance of the system has breached the constraints on the caution side, the verdict states that the system with its present performance still remains inadequate for solar testing purposes.

Although the steady-state parameters of the following two tests are measured to be acceptable in reference to 'interpretation two' of the standard [App. C], the steady-state responses in the next phase of result analysis will be solely examined in terms of their absolutes deviations from the mean and the cause of such large deviations.

9.4.2 Steady-state at 45°C

Figure 35 shows a 15 minute steady-state performance of the temperature measurements recorded at sample rate of once per second.

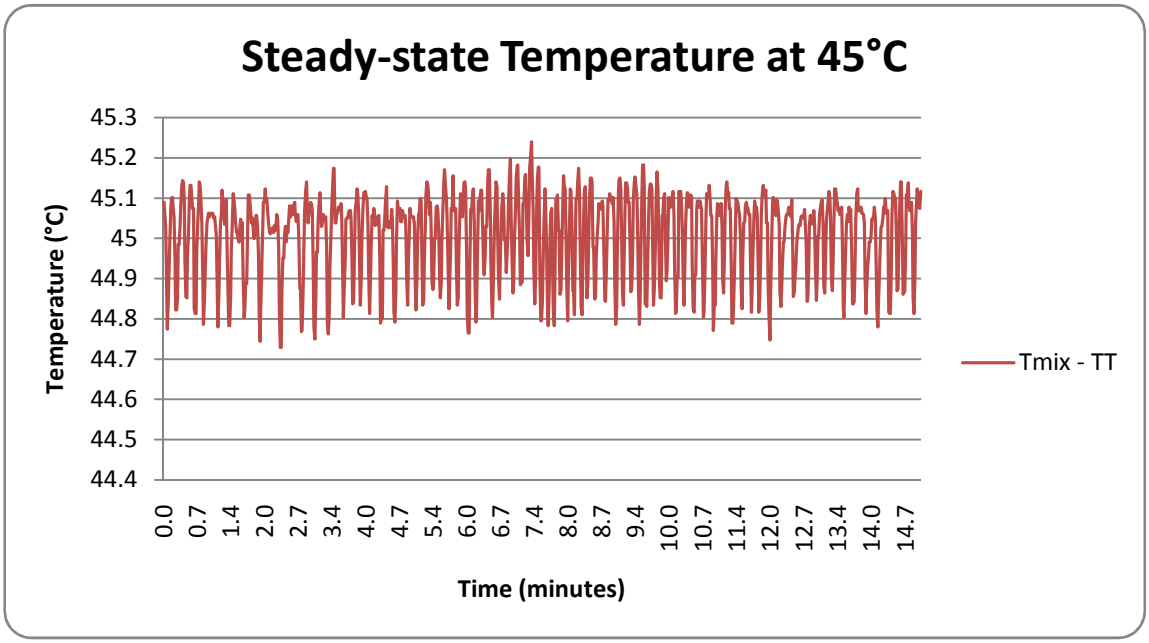

Figure 35: Steady-state temperature at 45°C

Steady-state temperature at 45°C	
Mean	45.006
Median	45.041
Standard Deviation	0.1
Maximum	45.239
Minimum	44.729
Range	0.51
Error ± (°C)	0.271

Table 12: Statistical data for steady-state temperature at 45°C

Although the steady-state results above managed a mean of 45°C, it contained a maximum error of ± 0.271°C which in fact exceeds the error measurement of the 30°C steady-state test. One issue realised from this response is the increase of oscillation magnitude from the previous response observed at 30°C. Due to the fact that the temperature response is directly determined by the flow-rate performance, the source of the magnitude increase must be explained through the behaviour of the flow-rate. Although it is necessary to identify which factor is responsible for the oscillatory action, this will be identified in due course.

Below in figure 36, is the response of the flow-rate to a 45°C steady-state test.

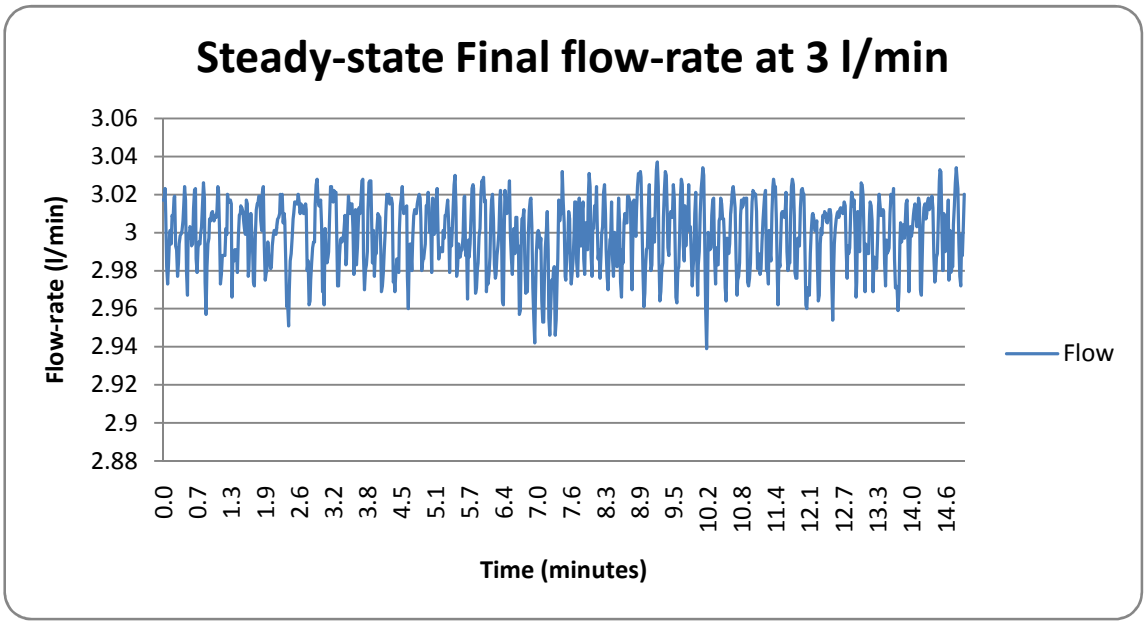

Figure 36: Steady-state Flow-rate for a 45°C inlet temperature

Steady-state Flow-rate at 45°C	
Mean	2.999
Median	3.001
Standard Deviation	0.018
Maximum	3.037
Minimum	2.94
Range	0.097
Error ± (l/min)	0.06

Steady-state Flow-rate at 30°C	
Mean	2.998
Median	2.997
Standard Deviation	0.014
Maximum	3.043
Minimum	2.953
Range	0.09
Error ± (l/min)	0.045

Table 13: Statistical data comparison between Steady-state Flow-rate at 45°C - 30°C

The results above reveal several instantaneous spikes in which the flow-rate reached an error of -0.06 l/min that is in fact twice the maximum magnitude permitted by the standard. However these spikes only occurred for small finite periods of time hence cannot be responsible for the increase in magnitude witnessed from the graph. It is interesting to see that the standard deviation of the flow at 45°C is very similar to standard deviation of the flow-rate at 30°C. This implies that the ultimate flow-rate performance has hardly declined at 45°C, yet an amplified temperature fluctuation occurs. The process to identify the issue responsible for the increase in magnitude must be examined through a deeper level by studying the behaviour of each flow stream in terms of control performance

Figure 37 and figure 38 represent the hot stream flow-rate control behaviours at 30°C and 45°C consecutively, over a steady state period of 200 seconds, sampling at once per second.

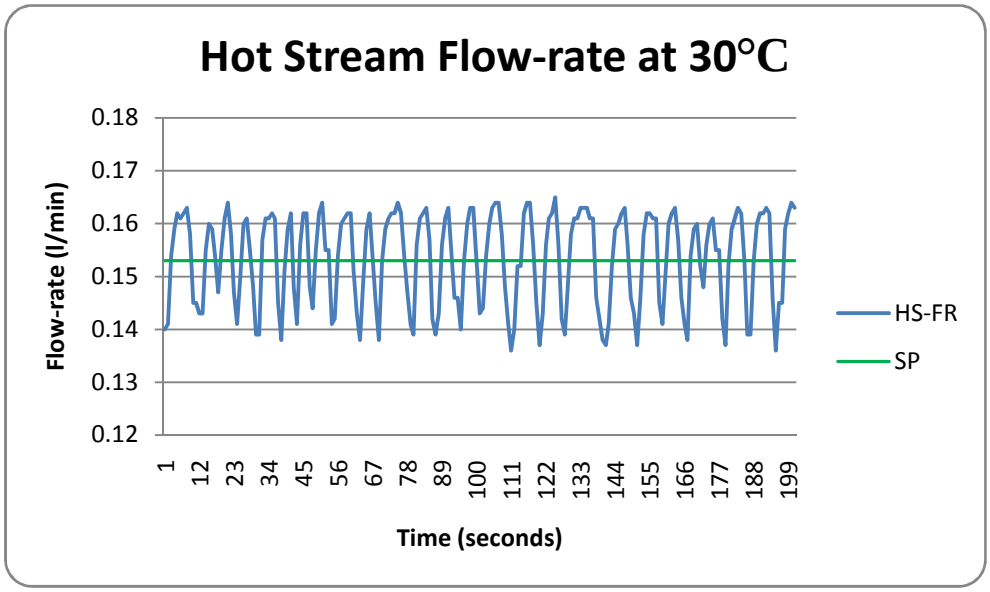

Figure 37: Hot stream Flow-rate at 30°C

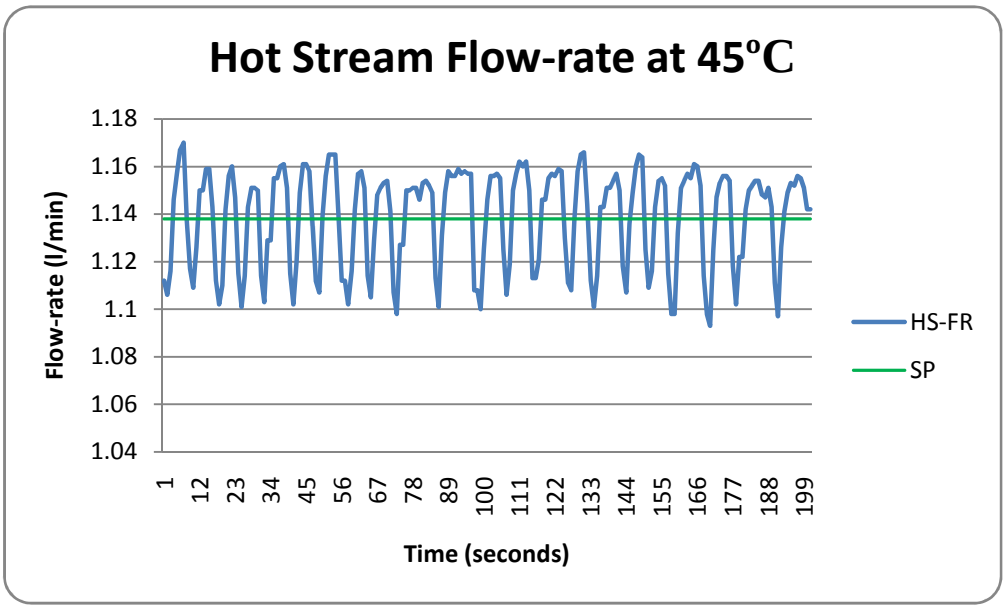

Figure 38: Hot Stream Flow-rate at 45°C

To achieve a final steady-state temperature of 45°C, a higher flow-rate is required from the hot stream in comparison to the required flow-rate at 30°C. Even though both streams oscillate evenly around their set-points from the de-coupler, the flow-rate deviation from the mean at 45°C is three times the amount at 30°C. This bounded amplification is believed to be accountable for the increased error in final temperature. The negative outcome presented from this control action could then cause damage to the control valves over a long term period as they are constantly ordered to open and shut.

9.4.3 Steady-state at 60°C

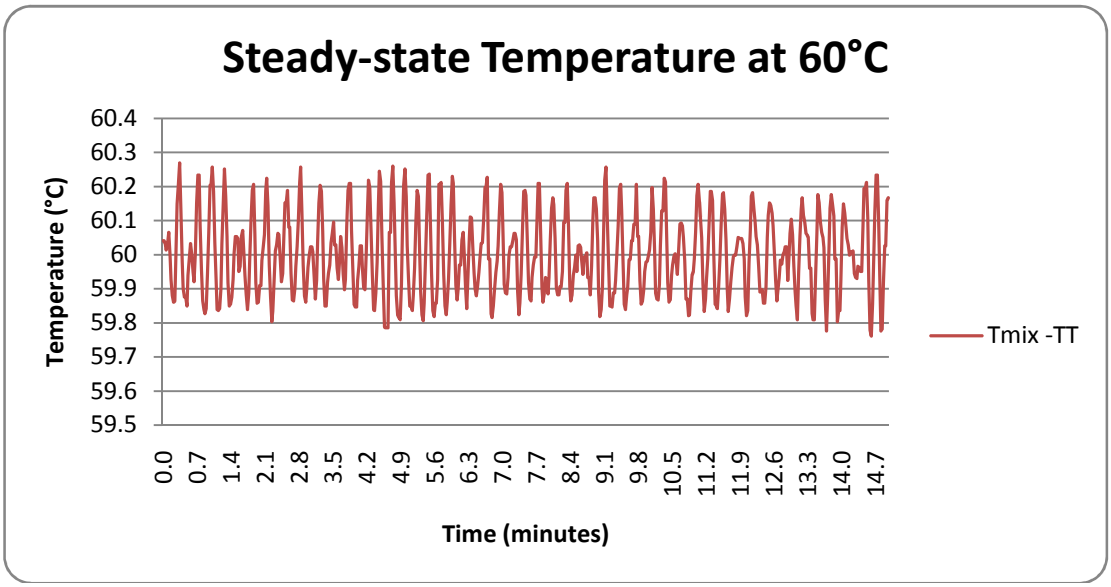

Figure 39: Steady-state temperature at 60°C

Steady-state temperature at 60°C	
Mean	60.001
Median	59.993
Standard Deviation	0.119
Maximum	60.269
Minimum	59.761
Range	0.58
Error ± (°C)	0.269

Table 14: Statistical date for Steady-state at 60°C

Once again, at a steady-state of 60°C, the temperature fluctuates violently within a range of 0.58°C. The steady-state temperature fluctuation for this test was vaguely larger than the test at 45°C for this same parameter. The cause of this rather immense variation in the temperature is once again due to the control performance of the hot stream flow as shown in figure 40 on the next page;

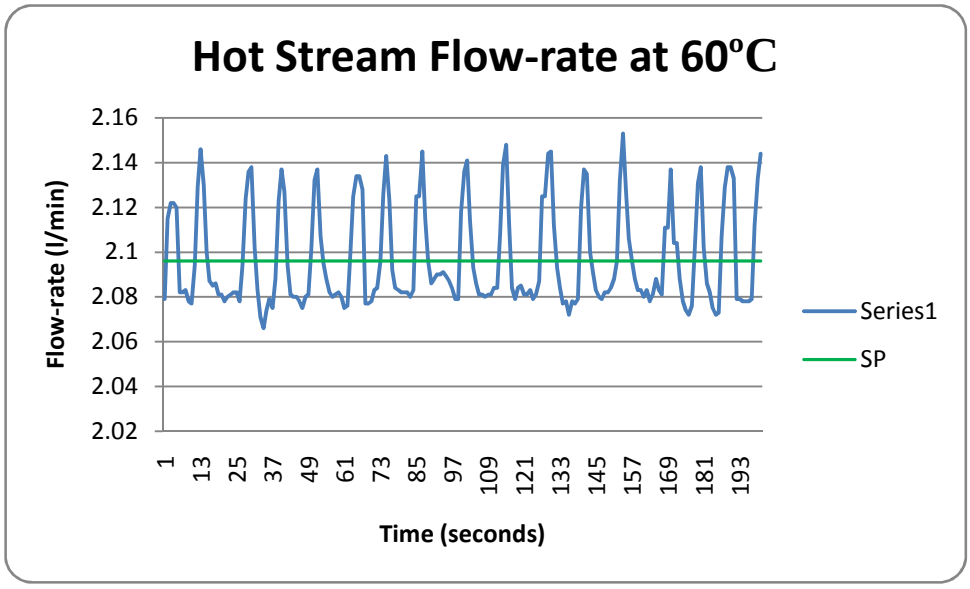

Figure 40: Hot stream Flow-rate at 60°C

For a hot stream flow-rate set-point of 2.09 l/min, the flow-rate still tends to fluctuate between a ± 0.03 l/min bound however the frequency of fluctuation has been reduced. This is once again believed to be due to an inaccurate control signal sent to the valve which provoked such large deviations. Figures 41 and 42 shown below, indicate how the valve was controlled at 30°C in comparison to the control performance at 60°C

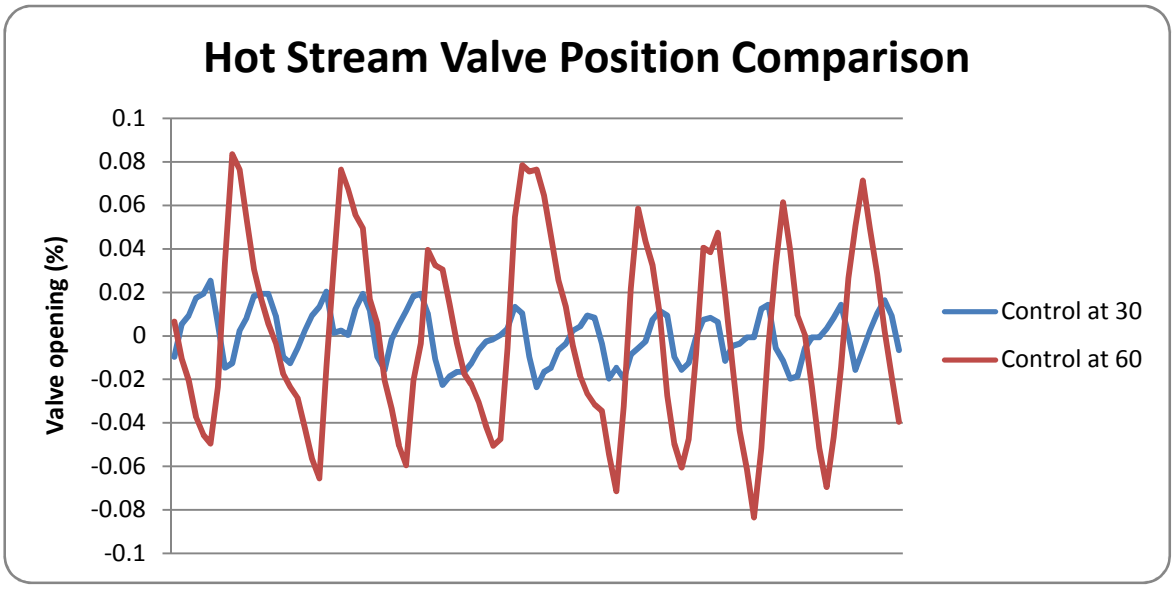

Figure 41: Hot Stream Valve Control for 30°C and 60°C

At a higher hot stream flow-rate, the controller tends to magnify the valve position bound which is completely unnecessary. In fact the magnitude of fluctuation at 60° was four times the amount at 30°C. Figure 42 shows how the controller handled the cold stream flow-rates for the same test.

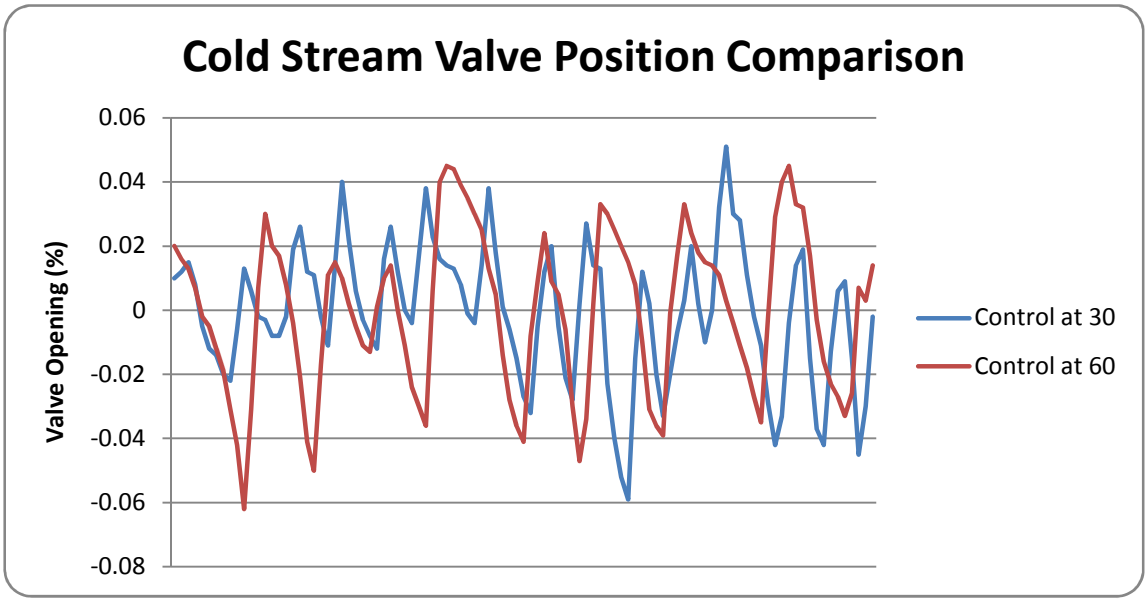

Figure 42: ColdStream Valve Control for 30°C and 60°C

Figure 42 suggests that the cold stream controller behaves the same for any given cold-stream flow-rate. The fluctuations above are in fact quite small, representing a few motor step intervals from either side of the set-point. However, since the control performance proved to accurately manage the hot stream flow-rate by a valve range of ± 0.02%, this in turn proves that there is still room for improvement in the control strategy.

Treating this matter is not trivial; however, it is suspected that the PID blocks currently used in the LabVIEW program may have some sort of programming glitches which are causing inappropriate control signals to be sent to the valves. Some future modifications must be considered around the control scheme to limit the bounds of the signals sent to the valves.

9.5 Open Loop System Oscillatory

After examining the system's steady-state results above, it was quite clear that the flow-rate responses incurred some form of oscillatory nature which was almost certainly responsible for the inadequate steady-sate accuracies. Therefore, if the source of the oscillatory motion was theoretically reduced or better yet removed, the system would stand a much better chance of satisfying the constraints of the caution side.

A simple open loop test was conducted on the stream flow-rates to determine the nature of the flow-rate signals. If the nature of the open-loop flow-rate signals were found to be noisy, then this would be consequently realised as a continuous flow-rate disturbance by the controllers. A continuous flow-rate disturbance implies that the controller must constantly act,

to compensate for the error. Therefore, this would ultimately depreciate the controller's performance in comparison to if the nature of the open-loop signals were identified to be 'smooth'.

The open loop test consisted of opening each valve to 30% with the water in the hot tank pre-heated to a temperature of 75°C and an ambient cold water temperature of 27°C in the cold water tank. This test discovers the raw signal nature of both stream flow-rates and the final temperature. The outcomes of this test are shown below starting with the steady-state measurements of the hot flow-rate signal.

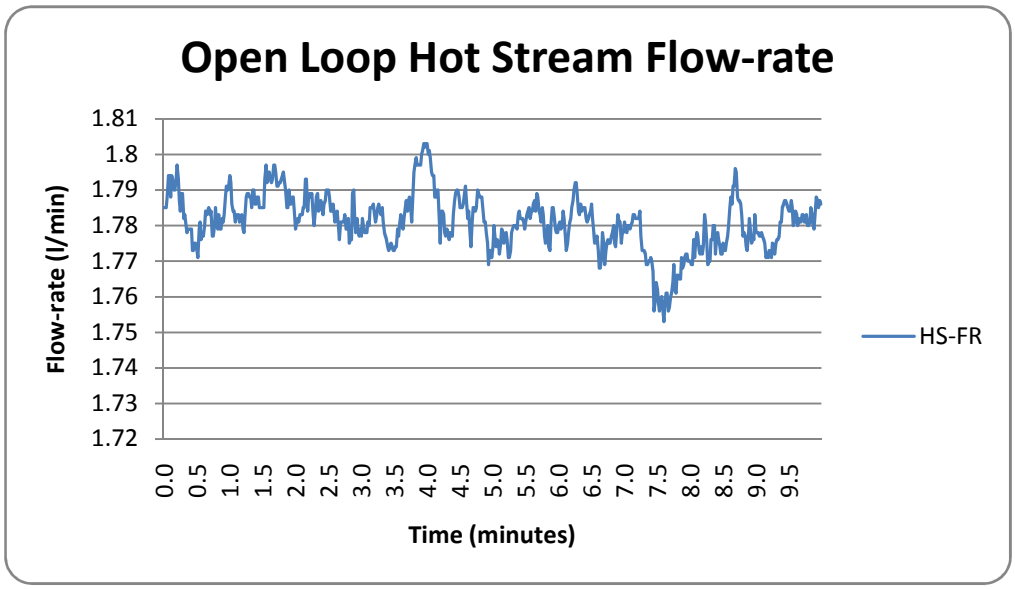

Figure 43: Open loop test for hot stream Flow-rate

As can be seen from the graph above, the raw signal exhibits some degree of fluctuation with the range recorded to be 0.05 l/min over the 10 minute period. The scattered measurements of this flow-rate could be due to these possible reasons:

1. Noisy signal
2. Slight fluctuation in the supply feed
3. Flow meters not mounted correctly

Most instrumentation signals exhibit noise which results from a variety of external interfering factors. Hence the probability that the signals are noisy is quite high. However, on the counter argument, both flow meters are earthed and the signal is deliberately passed through a current loop which is known to reduce the factor of noise. The possibility of slight

fluctuations in the supply feed is probable because the feed comes from a long pipe where constant pressure disturbances are prone to occur when other sources around the university site access water through this pipe. The probability that the flow meters were not mounted correctly is also unlikely because they were carefully mounted in a horizontal position and read off a full pipe.

Whatever the case may be, the quality of this signal is definitely of concern and therefore needs to be filtered out. One possible way to treat this issue is by passing the signal though a low-pass digital filter in the LabVIEW program. A low pass filter should be specifically employed because the signal only contains low frequency components.

The cold stream flow-rate signal was also logged and is revealed below in figure 44;

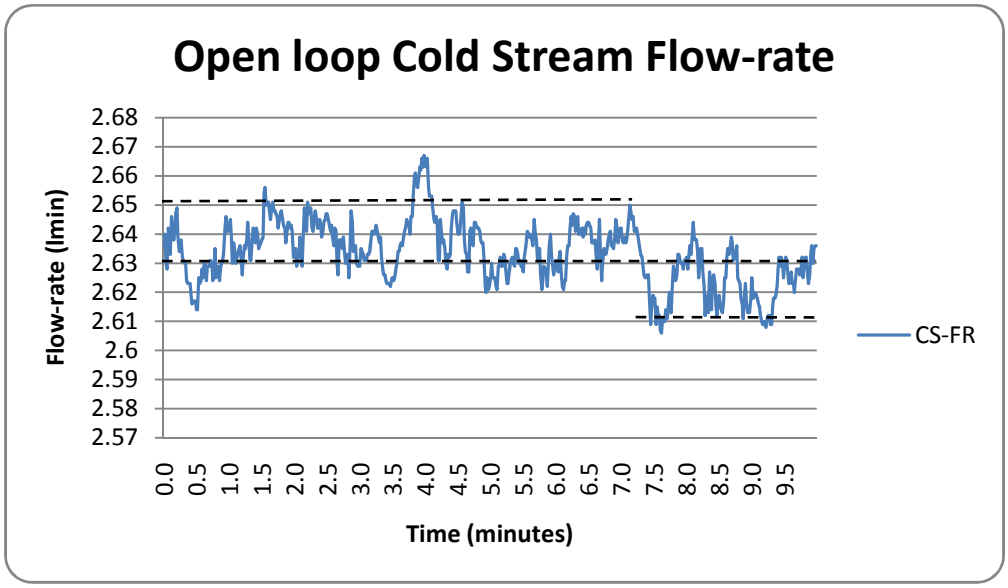

Figure 44: Open loop cold stream Flow-rate

This signal also behaves similar to the hot stream flow-rate in the sense that most fluctuations lay within the bound of ± 0.01 l/min from the mean as shown by the dotted lines above. This fact is also true for the hot stream flow-rate signal. However, it was also found that from day to day that these fluctuations varied in magnitude which made it difficult to distinguish if a certain error in the steady-state performance was due to a control glitch or a disturbance from this signal.

Below in figure 45, is the graphical representation of the resulting open loop temperature as a product of both streams;

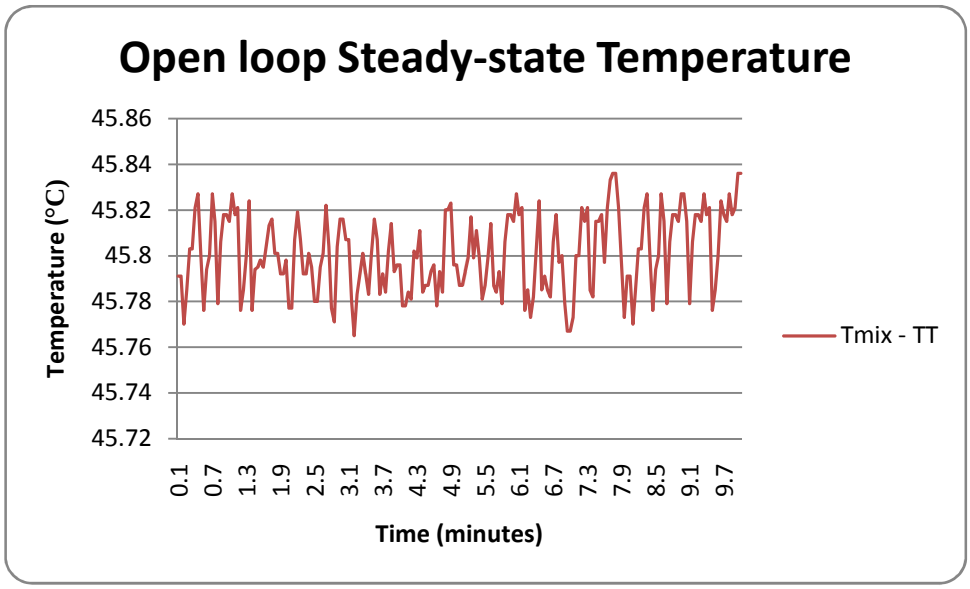

Figure 45: Open loop Steady-state temperature

Upon performing a quick calculation, the final mixed stream temperature is slightly below where it should, due to the heat losses from the pipes. However, this issue is cured by the additional PI controller, when the system is under control mode. It is interesting to note that the temperature oscillates steadily around a mean of 45.8°C with a deviation of ±0.02°C; this confirms that the system is capable of satisfying the steady-state rules of the standard, with its current measuring instruments. However, these open-loop tests have also indicated that the system's steady-state fluctuations in control mode are a product of both the control errors and the open-loop fluctuations.

10 PROJECT OUTCOMES AND FUTURE SUGGESTIONS

10.1 PROJECT OUTCOMES

This project was devoted to modifying a pre-existing system in aim to improve its accuracy performance to abide by the Australian and New Zealand Standard 'AS/NZS 2535.1:2007'. The project modifications made were:

- Implementation of Proportional control valves - Eliminated effects of pre-existing hysteresis
- Instrumentation calibration – Eliminated temperature off-sets between the RTD's
- LabVIEW loop time adjustment – Provided more accurate control performance
- Hot water tank Heater setting – To assure water in the tank doesn't drop past 70°C
- Additional PI loop around T_{Mix} – TT – Eliminated temperature offset in the mixed flow

A dramatic improvement has been made to the accuracy of the steady-state performance of the system in response to the modifications listed above. The elimination of the pre-existing valve hysteresis evidently caused the key development to the system's steady-state performance.

The ambiguity in the written structure of the AS/NZS document caused two sets of interpretations to be drawn in regards to how an acceptable system steady-state is to be determined. Although the system's performance comfortably satisfied the steady-state requirements of the standard by one of the possible interpretations, the steady-state performance was inclined to be tested under the stern assessment conditions of the opposing interpretation as a safety precaution. In that circumstance, the system was found to breach the steady-state accuracy limitations and for that reason, it is still presently judged to be an ineligible system to test a solar collector's efficiency.

The worst error in terms of the steady-state deviation from the mean value was measured to be ± 0.24℃ for the temperature parameter and ± 2% in terms of flow-rate. These error values were not consistent through the duration of the steady-state tests but were a result to possible surrounding disturbances.

The failure of the steady-state accuracies are believed to be due to two main reasons. The first suspicion is due to a control glitch from the hot stream flow-rate PI controller. The results lay evidence that PI controller illogically tends to amplify the fluctuations of the flow-rate at

set-point temperatures above 30℃. The second issue believed to be contributing to the accuracy deficiency of the system's performance, is the fluctuations of the open-loop steady-state flow-rate signals. Several speculations have been made to identify the cause of the irregular signals but luckily this can be easily treated. The text below highlights some future suggestions that may be carried out to solve these issues that were found to be prime suspects responsible for the steady-state performance failure.

10.2 FUTURE SUGGESTIONS

10.2.1 Open-loop signal

In terms of the open-loop signal fluctuations, there are two types of treatments that may be implemented to heal this issue. The first solution is to pass both the flow signals through a digital low-pass filter in the LabVIEW program. The intention of the low-pass filter is to smooth out the flow signals before any control operations are performed on them.

The second suggestion is to install a pressure gauge on the input supply feed to monitor the pressure variations. These variations can be sent to the Lab-view program as flow-rate disturbance signal. Therefore, a feed-forword control scheme can be implemented in the program to cancel out the incoming pressure disturbances from the supply feed to ultimately improve the control performance accuracy of the system.

10.2.2 Control glitches

The cause of the rather large valve fluctuations at steady-state temperatures above 30°C was not obvious after examining all the affecting factors which may have provoked the controller to increase the valve's positioning bounds. The current PID blocks used in the LabVIEW program were employed in substitution of the old PID blocks to allow for manual mode control. A growing suspicion is that the replacement PID blocks may contain some kind of embedded fault which could be responsible for inaccurate control calculations. Anyhow, some serious future considerations must be made to resolve this issue, starting by replacing all the current PID blocks with alternative blocks.

REFERENCES

Al-Senaid, HA. 2007 Solar Collector Efficiency Testing Unit, Murdoch University press.

Jian, E. 2006 *Solar Collector Efficiency Testing Unit, Murdoch University press*

ISO 9805-2:2007, *Test methods for solar Collectors – Part 2: Qualification test procedures, AS/NZS 2535.1:2007,* Standards Australia

Babatunde A. Ogunnaike, W. Harmon Ray, *Process Dynamics, Modelling and control.* Oxford University Press, 1994

EPV-250B owners manual, Hass manufacturing company, viewed 14th November 2008, http://www.hassmfg.com/manuals/epv.manual.pl/1235706283-76982.

Intellifaucet K series owner's manual*, Hass manufacturing company,* viewed 14th November 2008*, http://www.hassmfg.com/manuals/k.manual.pl/1235706283-76982*

PT-100 resistance table*, technical data sheets,* viewed 5th November 2008*, http://209.85.173.132/search?q=cache:hSwU8HQNoJ4J:whiteat.com/zbxe/%3Fmodule%3Dfile%26act%3DprocFileDownload%26file_srl%3D307%26sid%3D211457a580b8976f57bc30c4030fa8a4+pt-100+resistance+table&hl=en&ct=clnk&cd=1&gl=au*

Calibration, *Engineering Statistics Handbook,* viewed 15th November 2008, http://www.itl.nist.gov/div898/handbook/mpc/section3/mpc3.htm

Solar Thermal Collector, Wikipedia, http://en.wikipedia.org/wiki/Solar_thermal_collector viewed 14th November 2008.

APPENDIX A

FP WIRING DIAGRAMS

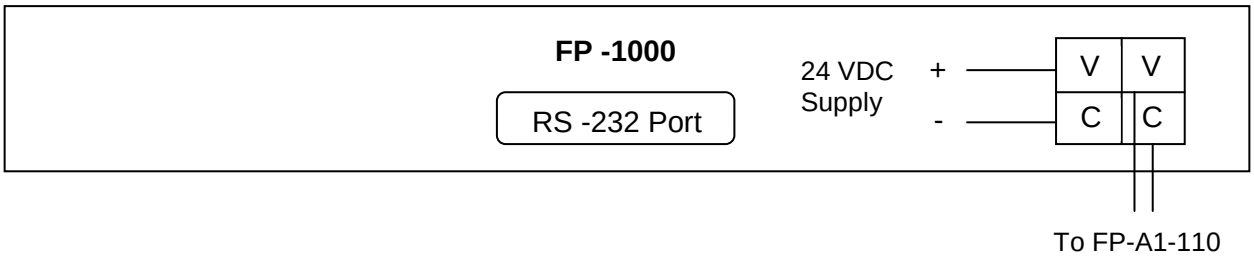

FP - AI - 110

V	1	2	3	4	5	6	7	8	9	10	11	12	13	14	15	16	V
C	17	18	19	20	21	22	23	24	25	26	27	28	29	30	31	32	C

Ch2: CT-TT

Ch5: HT-TT

To FP-A1-111

FP - AI - 111

V	1	2	3	4	5	6	7	8	9	10	11	12	13	14	15	16	V
C	17	18	19	20	21	22	23	24	25	26	27	28	29	30	31	32	C

Ch1: HS-FT

Ch2: HS-TT

Ch4: CS-TT

Ch6: T_{Mix}-TT

Ch7: CS-FT

To FP-AO-200

FP - AO - 200

V	1	2	3	4	5	6	7	8	9	10	11	12	13	14	15	16	V
C	17	18	19	20	21	22	23	24	25	26	27	28	29	30	31	32	C

Ch0: CS-CV

Ch1: HS-CV

To FP-A1-111

FP - PWM - 520

V	1	2	3	4	5	6	7	8	9	10	11	12	13	14	15	16	V
C	17	18	19	20	21	22	23	24	25	26	27	28	29	30	31	32	C

12 VDC

Ch0: To Hot Tank heater

APPENDIX B

STEADY-STATE RESULTS

Steady-state Temperature 45℃ – MEAN: 45.00608 (15 minutes)

Sample	1	2	3	4	5	6	7	8	9	10
Mean	44.990	45.013	44.994	44.981	44.998	45.014	45.002	45.009	45.009	45.004
Error (°C)	0.016	-0.007	0.012	0.025	0.008	-0.008	0.005	-0.003	-0.003	0.002

Sample	11	12	13	14	15	16	17	18	19	20
Mean	44.996	45.030	45.003	45.004	45.044	44.975	45.005	45.003	45.030	45.010
Error (°C)	0.010	-0.024	0.003	0.002	-0.038	0.031	0.001	0.003	-0.024	-0.004

Sample	21	22	23	24	25	26	27	28	29	30
Mean	45.018	44.993	45.004	45.014	44.994	44.994	45.018	44.997	44.999	45.021
Error (°C)	-0.012	0.013	0.002	-0.008	0.012	0.012	-0.012	0.009	0.007	-0.015

Table 15: Steady-state Temperature errors at 45℃

Steady-state Flow-rate at 45℃ – MEAN: 2.99903 (15 minutes)

Sample	11	12	13	14	15	16	17	18	19	20
Mean	3.000	3.001	3.000	2.999	2.998	3.002	2.999	3.001	3.000	3.002
Error (l/min)	-0.001	-0.002	-0.001	0.000	0.002	-0.003	0.000	-0.002	-0.001	-0.003

Sample	11	12	13	14	15	16	17	18	19	20
Mean	3.002	3.000	2.998	2.989	2.985	2.996	2.997	3.002	3.003	2.997
Error (l/min)	-0.003	0.000	0.001	0.010	0.014	0.003	0.002	-0.003	-0.003	0.002

Sample	21	22	23	24	25	26	27	28	29	30
Mean	2.997	3.000	3.000	3.000	2.993	3.003	3.000	2.996	3.006	3.005
Error (l/min)	0.002	-0.001	-0.001	-0.001	0.006	-0.004	-0.001	0.003	-0.007	-0.005

Table 16: Steady-state Flow-rate errors at 45℃

Steady-state Temperature 60℃ – MEAN: 60.00123 (15 minutes)

Sample	1	2	3	4	5	6	7	8	9	10
Mean	60.008	59.991	60.014	59.996	59.987	60.024	59.990	60.018	59.995	59.992
Error (°C)	-0.007	0.011	-0.013	0.005	0.015	-0.023	0.012	-0.017	0.006	0.010

Sample	11	12	13	14	15	16	17	18	19	20
Mean	60.008	60.017	59.996	60.009	60.014	59.992	60.008	60.008	60.000	59.982
Error (°C)	-0.006	-0.016	0.006	-0.007	-0.013	0.009	-0.006	-0.007	0.001	0.020

Sample	21	22	23	24	25	26	27	28	29	30
Mean	60.017	59.959	60.016	60.012	59.980	60.019	59.984	60.007	60.010	60.023
Error (°C)	-0.016	0.042	-0.015	-0.010	0.021	-0.018	0.017	-0.005	-0.009	-0.022

Table 17: Steady-state Temperature errors at 60℃

Steady-state Flow-rate at 60℃ – MEAN: 2.99950 (15 minutes)

Sample	1	2	3	4	5	6	7	8	9	10
Mean	3.005	2.997	3.001	3.000	2.994	3.007	2.995	3.006	2.995	3.002
Error (l/min)	-0.006	0.002	-0.001	-0.001	0.005	-0.008	0.004	-0.006	0.004	-0.003

Sample	11	12	13	14	15	16	17	18	19	20
Mean	3.000	3.003	3.002	2.999	3.004	2.995	3.002	2.999	3.000	2.997
Error (l/min)	0.000	-0.003	-0.003	0.001	-0.005	0.005	-0.003	0.000	-0.001	0.003

Sample	21	22	23	24	25	26	27	28	29	30
Mean	3.001	2.996	2.999	2.996	3.001	2.998	3.000	3.000	2.992	3.003
Error (l/min)	-0.002	0.003	0.000	0.003	-0.001	0.001	-0.001	0.000	0.008	-0.003

Table 18: Steady-state Flow-rate errors at 60℃

APPENDIX C

PID TUNING PARAMETERS

Ziegler Nichols

Controller Type	K_C	T_I	T_D
P	$\frac{1}{K}\left(\frac{\tau}{\alpha}\right)$	-	-
PI	$\frac{0.9}{K}\left(\frac{\tau}{\alpha}\right)$	3.33α	-
PID	$\frac{1.2}{K}\left(\frac{\tau}{\alpha}\right)$	2.0α	0.5α

Table 19: Ziegler Nichols Tuning Parameters

Cohen Coon

Controller Type	K_C	T_I	T_D
P	$\frac{1}{K}\left(\frac{\tau}{\alpha}\right)\left[1+\frac{1}{3}\left(\frac{\alpha}{\tau}\right)\right]$	-	-
PI	$\frac{1}{K}\left(\frac{\tau}{\alpha}\right)\left[0.9+\frac{1}{12}\left(\frac{\alpha}{\tau}\right)\right]$	$\alpha\left[\frac{30+3\left(\frac{\alpha}{\tau}\right)}{9+20\left(\frac{\alpha}{\tau}\right)}\right]$	-
PD	$\frac{1}{K}\left(\frac{\tau}{\alpha}\right)\left[\frac{5}{4}+\frac{1}{6}\left(\frac{\alpha}{\tau}\right)\right]$	-	$\alpha\left[\frac{6-2\left(\frac{\alpha}{\tau}\right)}{22+3\left(\frac{\alpha}{\tau}\right)}\right]$
PID	$\frac{1}{K}\left(\frac{\tau}{\alpha}\right)\left[\frac{4}{3}+\frac{1}{4}\left(\frac{\alpha}{\tau}\right)\right]$	$\alpha\left[\frac{32+6\left(\frac{\alpha}{\tau}\right)}{13+8\left(\frac{\alpha}{\tau}\right)}\right]$	$\alpha\left[\frac{4}{11+2\left(\frac{\alpha}{\tau}\right)}\right]$

Table 20: Cohen Coon Tuning Parameters

(Ogunnaike, 1994. Pg 536-537)

APPENDIX D

DEVICE DATA SHEETS + MANUALS

- **PT- 100 Resistance Tables**
- **EPV – 250B Proportional Control Valves**
- **Intellifaucet RK 250 Mixing Valve**
- **Promag 10 Flow Meters**
- **Davey Pumps**